의학박사 학위논문

Development of bispecific anti-proPSA × cotinine antibody for multiplex detection of proPSA using Raman signal

라만 신호를 이용한 proPSA 멀티플렉스 검출에 도입될 proPSA 와 코티닌 이중특이성항체의 개발

2016 년 2 월

서울대학교 대학원
의과학과 의과학전공
황 도 빈

라만 신호를 이용한 proPSA 멀티플렉스 검출에 도입될 proPSA 와 코티닌 이중특이성항체의 개발

지도 교수 정 준 호

이 논문을 의학박사 학위논문으로 제출함

2015년 10월

서울대학교 대학원

의과학과 의과학전공

황 도 빈

황도빈의 의학박사 학위논문을 인준함

2016년 1월

위 원 장 _____ (인)

부위원장 _____ (인)

위 원 _____ (인)

위 원 _____ (인)

위 원 _____ (인)

Development of bispecific anti-proPSA × cotinine antibody for multiplex detection of proPSA using Raman signal

by
Do Been Hwang

A thesis submitted to the Department of Biomedical sciences in partial fulfillment of the requirements for the Degree of Doctor of Philosophy in Biomedical sciences at Seoul National University College of Medicine

February 2016

Approved by Thesis Committee:

Professor _____Chairman

Professor _____Vice chairman

Professor _____

Professor _____

Professor _____

ABSTRACT

Introduction: A truncated precursor form of prostate-specific antigen (PSA), proPSA, is a well-known biomarker for prostate cancer. Since the amount of proPSA in serum or semen is quite low (1), it is impractical to purify it from biological fluid. Thereby, recombinant proPSA proteins must highly pure to use as a standard reference. For detecting [-2]proPSA and [-5/-7]proPSA in human serum, generation of selective and specific antibodies are essential. Based on reference materials and antibodies, an assay detecting [-2]proPSA and [-5/-7]proPSA in human serum simultaneously would offer a usefulness for detecting the prostate cancer.

Methods: In this study, proPSAs were expressed in HEK 293F cell and purified recombinant proteins from cell culture supernatant. Expressed proteins were identified by protein Edman sequencing and LC-MS/MS. The protein properties such as aggregation, monomeric or oligomeric forms and stability were analyzed by SEC-HPLC. After chicken immunization with identified proteins and propeptide-carrier protein conjugates, generation of polyclonal antibodies in

chicken serum was tested by immunoblot analysis. Bio-panning and phage ELISA using phage display technique, antibodies binding [-2]proPSA and [-5/-7]proPSA were individually developed.

The bispecific antibodies composed of 2 scFvs linked with human Fc domain were expressed in HEK 293F cells and purified by protein A beads. The characteristics of single walled carbon nanotube with bispecific antibody (SNA) were tested by Raman specrometry and BIAcore assay. The sensitivity and selectivity of SNA were analyzed by Raman imaging.

Results: In the developed expression and purification system, [-2]proPSA and [-5/-7]proPSA were generated stably, and production yields of recombinant proteins were approximately 585.6 μg/L, 522.2 μg/L, respectively. The antibodies targeting [-2]proPSA, [-5/-7]proPSA were developed form phage libraries constructed form chickens immunized with peptide conjugates or recombinant proteins. The screened out antibodies specifically bound to target proteins without cross-reactivity to other proteins and peptides in ELISA and immunoblot analysis.

An interaction between cotinine on synthesized SNAs and anti-cotinine antibody in a bispecific antibody was confirmed in Raman specrometry and BIAcore assay. In Raman imaging, it was proved that SNAs complexed with anti-HER 2 × cotinine antibody attached selectively on HER2 molecules on SK-BR-3 cell surface.

Conclusions: Taken together, [-2]proPSA, [-5/-7]proPSA were generated purely in developed system, and antibodies for [-2]proPSA and [-5/-7]proPSA were discovered from immunized chicken libraries. SNAs with bispecific antibodies were synthsized well and it's characteristics were confirmed by Raman spectroscopy and imaging. Based on developed materials such as recombinant proPSAs as the reference material, anti-proPSA antibodies and SNA with bispecific antibody, the assay detecting [-2]proPSA and [-5/-7]proPSA simultanously in a single tubes contaning human serum is under developing. If the assay is developed in near future, it could offer a usefulness for detecting the prostate cancer

* These works are published in Biotechnology and applied

Biochemistry(2), and Nanoscale(3).

Keywords: proPSA, prostate cancer, cotinine, antibody, SNA, Raman

Student number: 2008-23299

CONTENTS

Abstract 1
Contents 5
List of tables and figures 6
Overview 9

Chapter 1. Development of proPSA antibody
Introduction 17
Material and Methods 25
Results 33
Discussion 55

Chapter 2. Antibody and Raman imaging
Introduction 59
Material and Methods 64
Results 70
Discussion 79

References 82
Abstract in Korean 93

LIST OF FIGURES

Chapter 1

Figure 1. Prostate specific antigen biosynthesis.....20

Figure 2. Overall process of antibody geration from construction of antibody library to selection of antibody clones.....24

Figure 3. Overexpression and purification of recombinant [−2], [−7]proPSA, and PSA.....40

Figure 4. N−terminal sequencing of recombinant proteins 42,43,44

Figure 5. LC−MS/MS of recombinant proteins..... 45,46

Figure 6. SEC−HPLC of recombinant proteins.....47

Figure 7. Stability test of recombinant proteins..... 48,49

Figure 8. Epitope mapping of antibodies against [−2]proPSA and [−5/−7]proPSA protein.....51

Figure 9. The specificity test of 2pro6P antibody 53

Chapter 2

Figure 10. The construction of bispeicific antibody and SNA 63

Figure 11. Binding test of bispecufuc antibodies.....75

Figure 12. Raman spectroscopy of SNAs. 76

Figure 13. SPR sensorgrams for the binding of SNA and SWNT bioconjugates to HER2. 77

Figure 14. Selective detection of HER2-overexpressing cancer cells with SNA 78

LIST OF ABBREVIATIONS

proPSA : precursor prostate specific antigen

PSA : prostate specific antigen

PCa : prostate cancer patient

ACT : alpha-I-antichymotrypsin

A2M : alpha-2-macroglobulin

KLK : kallikrein

BPH : benign prostatic hyperplasia

ROC-AUC : receiver operating characteristic-area under the curve

RT-PCR : reverse transcription polymerase chain reaction

scFv : single chain fragment variable

V_H : variable heavy chain

V_L : variable light chain

SWNT : single walled carbon nanotube

SNA : bispecific antibody attaching SWNT by antigen-antibody interaction

SWNT biocinjugate : SWNT conjugated with bispecific antibody by EDC coupling

Cot : cotinine

OVERVIEW

The level of proteins existing in human surum is used as indicators for detecting an existence or progression of cancers. The measurement of protein biomarkers offers an enormous potential for detecting an early statge of cancers and monitoring of treatment outcomes (4). Among protein biomarkers in human serum, prostate specific antigen (PSA) have been a useful clinical biomarker for diagnosing the prostate cancer in several decades ago. PSA is a member of the tissue kallikrein family, located on chromosome 19q13.4 (5). Kallikreins are serine proteases digesting certain high molecular-weight proteins to release bioactive peptides termed kinins. The gene encoding hK1 (KLK1) is closest to the centromere and followed by KLK15, KLK3 (encoding PSA), and KLK2. The kallikrein genes are expressed in variety tissues, and many of them are regulated by steroid hormones. The PSA, hK2 and hK4 are expressed in prostate and regulated by androgen (6, 7). The close linkage of KLK2, KLK3, and KLK4 indicates that common prostate-specific regulatory elements (androgen-responsive elements) might control their expression. The PSA is a glycoprotein produced by the epithelial component of the

prostate gland (8). Men with prostatic diseases, including adenocarcinoma of the prostate, have high serum PSA levels due to over-production and architectural distortions in the gland (9). Most of the PSA in blood is complexed with various inhibitors including alpha-1-antichymotrypsin (ACT). The unbound form of PSA, known as free PSA, is present in three major molecular forms, i.e., inactive PSA (iPSA), benign PSA (BPSA), and proPSA (10).

The Food and Drug Administration has approved a blood test to measure elevated total PSA level for detecting prostate cancer at early stage and monitoring patients after an radication therapy for prostate cancer or prostatic surgery. Normal levels of PSA is typically 0.5 to 2 ng/mL and patents with an early stage prostate cancer have levels of 4 to 10 ng/mL. PSA serum concentration with 4 to 10 ng/mL is known as the gray zone, the level indicating the possibility of early stage prostate cancer. Late stage prostate cancer is characterized by values of 10 to 1000 ng/mL (11). Because the traditional threshold level of PSA is 4 ng/mL, an increasement of PSA level promptes a recommendation that the man undergo prostate biopsy (12). As PSA test is affected by prostatic hyperplasia, prostatitis, age,

race and personal variation, the PSA test is used as a suboptimal method for detecting early stage of prostate cancer. As an example, about 75% of men with the PSA levels of 4.0 to 10 ng/mL who undergo a prostate biopsy and they do not have cancer. To increase a specificity of the PSA test, many methods including age-specific PSA reference ranges (13), adjusting the PSA level to account for the volume or density of a prostate measured ultrasonographically(14), PSA velocity (PSAV)(15), PSA density (PSAD) (16), and free-to-total PSA ratio (%fPSA) have been proposed (17).

Among them, %fPSA and age-specific PSA cutoffs enhance the specificity of total PSA for cancer detection in men with PSA values between 4 and 10 ng/mL. %fPSA represents significantly higher sensitivities than age-specific PSA cutoffs in men older than 60 years of age (18). %fPSA could help distinguish between prostatitis and cancer, and it offers clinical utilities in men whose total serum PSA concentration is 2.5-10 ng/mL (19, 20). Also, %fPSA is helpful in selecting patients representing elevated total PSA level whether they need biopsy or not after initial negative biopsies (21). There is a study screening volunteers, age 50 years and older, whose total PSA

levels were 4.1−10.0 ng/mL and digital rectal examinations were not suspicious for prostate cancer. In this study, a cut−off value with 23% fPSA would have detected 90% of cancer and eliminated 30% of negative biopsies. %fPSA would help to avoid unnessasery biopsy, but an issue with a probability of cancer is still remained.

Because tPSA and %fPSA test represent unclear thresholds in aspects of specificity and sensitivity for the early detection of prostate cancer, many efforts are being made to discover new prostate specific markers. A truncated form of precursor of PSAs called proPSAs are new markers that are introduced to improve the accuracy of the PSA test (22). Native proPSA contains additional 7 amino acids named as pro−peptide in N−terminus of PSA, and proPSA isoforms with different lengths of pro−peptides are found in human serum (23). The proPSAs are highly expressed in prostate cancer and [−2]proSPA (p2PSA) among proPSAs is appear to correlate with prostate cancer. In the current study, %p2PSA ([−2]proPSA/fPSA×100) and prostate health index (PHI, (p2PSA fPSA)×$PSA^{1/2}$) based on [−2]proPSA level in serum represented the most accurate prediction of the presence of prostate cancer (24). When tPSA

threshold of 3.18 ng/mL showed a sensitivity of 90.1% with a PPV of 44.1%, but, same criteria (sensitivity of 90.1%), a threshold of 1.20 for %p2PSA and 25.5 for PHI (respective specificity of 37.9% and 23.0%) showed the best PPV (54.2 and 48.9%, respectively). It is indicate that %p2PSA and PHI could be an effective screening tool for diagnosing prostate cancer (25).

As [−2]proPSA existing in human serum with picograms per millilitre, a powerful tool with a high sensitivity is needed. The highly sensitive immunoassay with various signal amplification strategies coupled with nanomaterials have been developed as novel tools and platforms for biomedical research and applications(26). Carbon nanotubes (CNTs) are remarkable nanomaterials and defined as allotropes of carbon with cylinders of graphene sheets (27). Wang et al. investigated their novel applications by using CNTs as labels for ultrasensitive electrochemical immunoassays (28). In the study, CNTs could load numerous enzyme tracers via chemical reactions on their long surface. The numerous enzyme−loaded CNT super labels were applied for the magnetic beads−based immunoassay, and a detection limit of the assay was 50−150

fg/mL. A signal enhancement was around 100-fold than a system consisting of a single-enzyme label. Hence, CNTs could be useful probes in signal-enhanced immunoassay for detecting low-level of proteins in human serum. CNTs are classified as a single layer of graphene sheet (single-walled CNT; SWNT)(29) and cylinderic muli-layers form (multi-walled CNT; MWNT)(30). MWCNTs are usually generated with diameters in the range of 1-3 nm for the inner tubes and 2-100 nm for the outer tubes (31). The SWNT have diameters of 1-2 nm, and lengths ranging from as short as 50 nm up to 1 cm (32).

In near-infrared (NIR) light, SWNTs exhibit a strong resonance Raman scattering through their electronic density of states at the van Hove singularities (33). SWNTs represent several distinctive Raman scattering including the radial breathing mode (RBM) and tangential mode (G-band) (34). RBM and G-band demonstrate a sharp and strong peak which could be distinguishable from a noise or background. Because of the physiological properties of SWNTs generating a strong and intrinsic Raman spectra (35), SWNTs show a large shift of peaks compared with traditional fluorescence reagents. Chen et al. reported that they developed an immunoassay using

functionalized SWNTs and detection limit of the assay was 1 fmol/L, approximately three orders of magnitude than commonly used fluorescence assay (36). Moreover, SWNTs could be synthesized with different isotope compositions exhibited different G band peaks, and thus it could be used as multicolor contrast agents for multiplexed Raman imaging. Zhuang et. al (37) reported that three kinds of SWNTs labeled with different isotope compositions were sucessfully synthesized and conjugated with three ligands such as Herceptin (anti-Her2), Erbitux (anti-Her1), and RGD peptide, respectively. In confocal Raman imaging, it was confirmed that functionalized SWNTs selectively bound cancer cells expressing a specific recpetor. Raman signals of SWNTs rarely photobleached even under high excitation powers, hence SWNTs are promising materials for biosensing and biomedical imaging (38).

CHAPTER 1

Development of proPSA antibody

INTRODUCTION

Precursor Prostate specific antigen (proPSA)

Prostate-specific antigen (PSA) is a glycoprotein produced by the epithelial component of the prostate gland (39). Men with prostatic diseases, including adenocarcinoma of the prostate, may have high serum PSA levels due to its enhanced production and architectural distortions in the gland that allow PSA to enter the circulation (40). It was well known that several forms of PSA exist in blood and seminal fluid. Most of the PSA in blood is complexed with various inhibitors including alpha-1-antichymotrypsin (ACT). The unbound form of PSA, known as free PSA, is present in three major molecular forms, i.e., inactive PSA (iPSA), benign PSA (BPSA), and proPSA (41).

PSA is also one of the few organ-specific markers routinely used to detect cancer and monitor the effectiveness of treatment or progression. Men with serum PSA levels above 10 ng/mL have a 50% or higher chance of developing prostate cancer (42). Use of the PSA test has increased early detection of prostate cancer (43, 44). Despite the overall success of this test, its use is limited by a lack of specificity, especially in men with a total PSA (tPSA) level of <10 ng/mL. Patients with this

level of serum tPSA frequently harbor both benign and malignant prostatic conditions (45, 46). Men with PSA levels between 4–10 ng/mL are considered candidates for prostate biopsy to confirm the presence of cancer. However, one study showed that only 20–40% of men within this range have prostate cancer (47).

A truncated form of precursor of PSA called [−2]proPSA is an additional marker that was introduced to improve the accuracy of the PSA test. The [−2]proPSA was found to be overexpressed in malignant cells relative to benign prostate cells, as well as significantly elevated in serum of men with prostate cancer (48). In the large multicenter prospective study, percent [−2]proPSA ([−2]proPSA/freePSA) showed clinical value (49). At a fixed sensitivity of 80%, percent [−2]proPSA showed higher specificity (51.6%) than PSA (29.9%) in the 2−4 ng/mL PSA range. In the PSA range of 2−10 ng/mL, its specificity was 44.9% while the PSA test showed 30.8% specificity (49). It is generally agreed that percent [−2]proPSA differentiates between prostate cancer and benign prostate disease when the tPSA level is in the 2−10 ng/mL range (49−51). In another study, percent [−2]proPSA was

significantly higher in patients with a higher Gleason score and more aggressive cancers (49). Taken together, these findings indicate that [−2]proPSA can be a potential biomarker not only for the accurate detection of prostate cancer but also for determining prognosis.

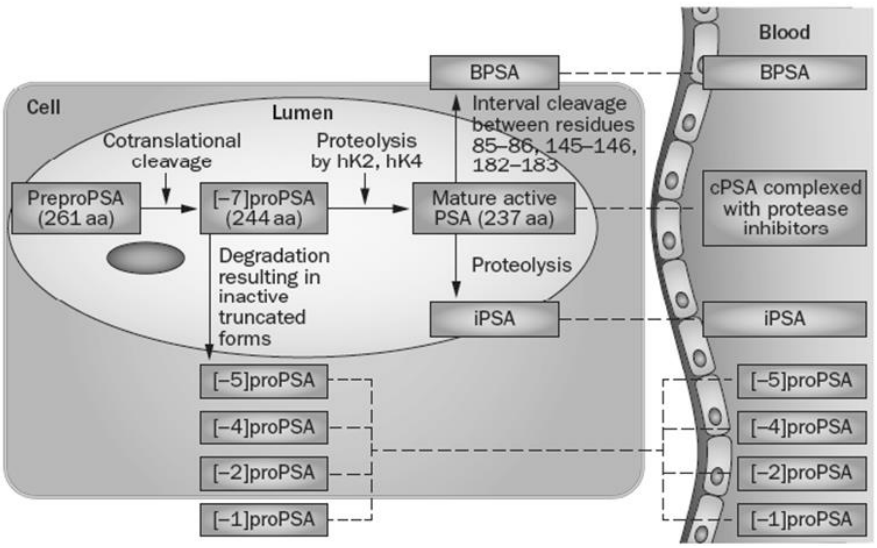

Figure 1. Prostate specific antigen biosynthesis

Phage display

Phage display refers to the display of functional foreign peptides or small proteins on the surface of bacteriophage. Phage display technology was introduced in 1985 by George P. Smith (52). He showed that foreign DNA fragments could be inserted into filamentous phage genome, which initiated the new technology of phage display (52). Phage genome is a single-stranded DNA that is encased in coat proteins, i.e., the major coat protein, pVIII, (with about 2700 copies per phage) and minor coat proteins, pIII, pVI, pVII and pIX (each with five copies per phage). Bacteriophages propagate within bacterial hosts upon infection. The phage takes over the hosts' biosynthetic machinery to produce all the necessary enzymes for phage protein production and replication of phage genetic materials for subsequent phage assembly. Each infected bacterial cell can produce over a thousand of identical phage particles.

Filamentous phage was first used to display small peptides, other proteins and antibodies by fusion to the minor coat protein, pIII (53, 54). The antibody fragment can be displayed as single chain Fv fragment which is composed of VH domain, a

flexible linker and VL domain in order (55, 56). Also, it could be displayed as Fab fragment, in which one chain is fused to pIII and the other is secreted into the periplasm (57-60). When antibody fragments are fused to the N-terminus of pIII, the phage maintain their infectiveness. However, if the N-terminal domain of pIII is excised for making the second domain, the phage loss their infectiveness. In this case, wild type pIII must be provided by helper phage (61, 62). The major coat protein of the phage, pVII, can also be used to display peptides (63-65) and antibody fragments (66, 67). Pentapeptides (63) and hexapeptides (64) could be fused close to the N-terminus of pVIII, but the phage encoding longer peptides did not generated unless wild type pVIII was provided (68). Therefore, pIII rather than pVIII have been preferred for antibody display.

Bio-panning

Bio-panning is the procedure of selecting binding pairs from phage display libraries. Antibody displaying phage particles are incubated with the immobilized antigen coated plates (69), column matrices (57), cells (70), or to biotinylated antigen in solution followed by capture (71). After incubation, non-

specific phages bound to the solid phase are removed by washing steps, and then phages attaching antigens by antigen and antibody interaction on the solid phase are eluted by acid (69) or alkali (72). The eluted phages are used to infect E. coli and subsequently re-amplified for further rounds of selection. This selection cycle is commonly carried 4 or 5 times until satisfactory enrichment achieved. The overall process is shown in Figure 2 . Phages can be enriched 20-1000 fold by a single round of selection (73, 74). In this way, enrichment factors of only 50-fold in each round can build up to 10^7-fold enrichments over four rounds of selection (72). Bio-panning based on phage display technology most widespread method for developing antibodies and for the engineering of selected antibodies. It is highly versatile method to isolate high-affinity human antibodies from nonimmune and synthetic libraries (75-77). Moreover, it offers an opportunity for developing picomolar affinity antibodies by affinity maturation (78), and discover antibodies with unique properties from nonimmune and immune libraries from animal or human donors (79).

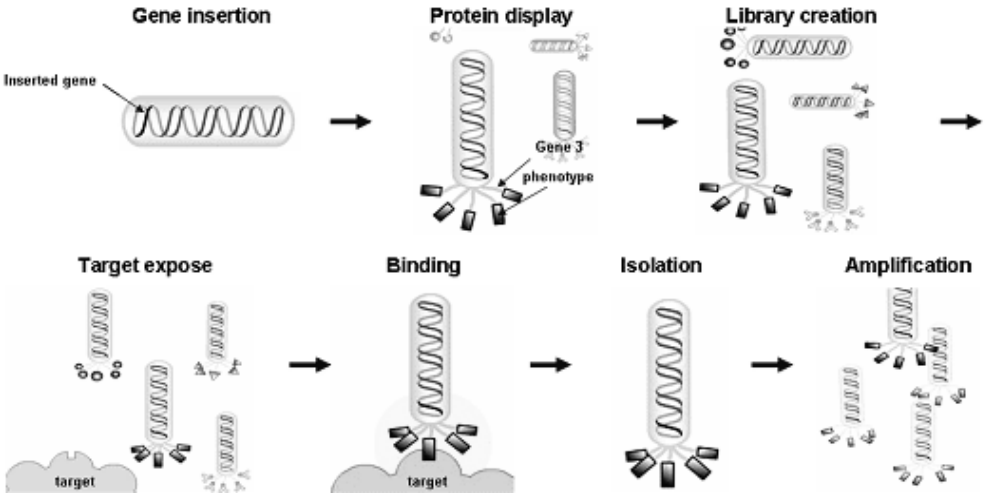

Figure 2. Overall process of antibody generation from construction of antibody library to selection of antibody clones

MATERIAL AND METHODS

1. Establishment of expression vectors and the expression of recombinant proteins

The proPSA cDNA was purchased from the Korea Research Institute of Bioscience and Biotechnology (KRIBB). The genes encoding [−2]proPSA, [−7]proPSA, and PSA were isolated by PCR using 5'−CCCAAGCTTATGTGGGTCCCGGTTGTCTTCC TCACCCTGTCCGTGACGTGGATTGGCGCTGCGCCCCTCATCC TGTCTCGG−3',5'−CCAAGCTTATGTGGTCCCGGTTGTCTTC CTCACCCTGTCCGTGACGTGGATTGGCGCTTCTCGGATTGT GGGAGGCTGG−3', and 5'−CCCAAGCTTATGTGGGTCCCGG TTGTCTTCCTCACCCTGTCCGTGACGTGGATTGGCGCT ATT GTGGGGGCTGGGAGTGC−3' with HindIII restriction site (underlined) as reverse primer, respectively, and 5'− CTGGCCGGCCTGGCCGGGGTTGGCCACGATGGTGTC−3' with SfiI restriction site (underlined) as a forward primer. The amplified genes were digested with HindIII and SfiI restriction enzymes (both from New England BioLabs, MA, USA) and ligated into a pCEP4 expression vector (Invitrogen, CA, USA) which was modified to contain the human C_{κ} domain using T4 DNA ligase (Invitrogen) as reported previously (80).

HEK 293F cells (Invitrogen) were cultured in GIBCO FreeStyleTM 293 Expression media containing 10,000 IU/L penicillin and 100 mg/L streptomycin (Invitrogen) at 37 ℃ in an orbital shaking incubator (Minitron, INFORS HT, Bottmingen, Switzerland) with 7% CO_2 at 135 r.p.m. Cells were transfected with the pCEP4 expression vectors using 25 kDa linear polyethylenimine (Polysciences, PA, USA) as described previously (81). After 5 days of culture, the culture supernatant was subjected to affinity chromatography using KappaSelect resin (GE Healthcare, London, UK). The recombinant proteins were purified according to the manufacturer's instructions.

2. Synthesis of peptide conjugates

Peptides representing the N-terminal sequence of [-7], [-5], and [-2]proPSA, namely APLILSRIVGGWEC (7pro), LILSRIVGGWEC (5pro), and SRIVGGWEC (2pro), respectively, were chemically synthesized by Peptron Inc. (Yuseong-gu, Daejon, Korea). The synthesized peptides were conjugated to bovine serum albumin (BSA), keyhole limpet hemocyanin (KLH), or ovalbumin (OVA) as described previously.

3. Gel electrophoresis and immunoblot analysis

The recombinant proteins or peptide-BSA conjugates were resolved by SDS-PAGE using NuPage 4-12% Bis-Tris gels (Invitrogen) according to the manufacturer's instructions. To visualize protein bands, the gel was subjected to Coommassie Blue staining as described previously (82).

For immunoblot analysis, the proteins were transferred to nitrocellulose membrane as described previously (83). Then the membrane was blocked with 5% skim milk (BD Biosciences, CA, USA) in TBS containing 0.2% Tween-20 (TBST) at room temperature for 1 h. After blocking, the membrane was incubated with the D6B1 and D11E1 antibodies (Cell Signaling Technology, MA, USA) diluted 1:2,000 in 5% skim milk/TBST for 12 h at 4 ℃. After washing three times with 0.2% TBST, the membrane was probed with HRP-conjugated anti-rabbit IgG (Fc-specific) antibody (anti-rabbit Fc-HRP) (Abcam, Cambridge, UK) diluted in 5% skim milk/TBST at 37 ℃ for 1 h. In parallel, the membrane was subjected to extended blocking procedures without incubation with anti-PSA antibody and but only with HRP-conjugated anti-human C_{κ} antibody (anti-human C_{κ}-HRP) (Millipore, MA, USA) or anti-rabbit Fc-HRP

diluted in 5% skim milk/TBST at 37 ℃ for 1 h. Afterwards, the membrane was washed again with 0.2% TBST and was visualized by SuperSignal Pico West chemiluminescent substrate (ThermoFisher Scientific, IL, USA) according to the manufacturer's instructions.

To test the specificity of the anti-[-2]proPSA antibody (2pro6P), the membrane was sequentially incubated with anti-[-2]proPSA scFv-hFc fusion protein (2pro6P scFv-hFc) and HRP-conjugated anti-human Fc antibody (anti-human Fc-HRP) (ThermoFisher Scientific) with intermittent washing as described above. In a parallel experiment, the membrane was sequentially probed with D6B1 and anti-rabbit Fc-HRP and visualized as described above.

4. N-terminal sequencing of recombinant proteins

N-terminal sequencing of the recombinant proteins purified from the culture supernatant of HEK 293F cells transfected with expression vector encoding [-2]proPSA, [-7]proPSA, and PSA fused with human C_{κ} domain was performed by e-MASS (Guro-gu, Seoul, Korea) with ABI 492 protein

sequencer as described previously (84). The first five residues at the N-terminus were identified.

5. Mass spectrometry of recombinant proteins

Liquid chromatography coupled to tandem mass spectrometry (LC-MS/MS) of [-2]proPSA, [-5/-7]proPSA, and [+4]PSA fused with human C_{κ} domain wasereas performed byby e-MASS with AB SCIE TripleTOFTM 5600 which is a tool for measuring analizing molecular weight as described previously (85).

6. Size exclusion chromatography of recombinant proteins

To check the percentage of protein aggregation, size exclusion chromatography was performed by high performance liquid chromatography (SEC-HPLC). SEC-HPLC of [-2]proPSA-C_{κ}, [-5/-7]proPSA-C_{κ}, and [+4]PSA-C_{κ} protein was performed by Abclone (Guro-gu, Seoul, Korea) with Agilent 1260 as described previously (86).

7. Stability test of recombinant proteins

Thirty μg of [−2]proPSA−$C_κ$, [−5/−7]proPSA−$C_κ$, and [+4]PSA−$C_κ$ were prepared in 1.5 mL microcentrifuge tubes. The tubes were placed in deep freezer at −80 ℃ for 16 h and then samples were thawed at 4 ℃ . After the recombinant proteins underwent 1, 5 and 10 times of freezing and thawing process, percentage of protein aggregate in samples was analyzed by Abclone with SEC−HPLC as described previously (87).

8. Generation of antibody library from immunized chickens

Three white leghorn chickens were immunized and boosted three times with 5 μg of peptide−KLH or peptide−OVA on an alternating basis by BioPOA Inc. (Gwonsun−Gu, Suwon, Korea). Blood was collected from the wing vein two weeks after each immunization or boost.

A phage display library of single−chain variable fragments (scFvs) was constructed using total RNA isolated from the harvested spleen, bone marrow, and bursa of Fabricius of the immunized chickens, as described previously (88). A total of five rounds of biopanning were performed as described previously using magnetic beads conjugated with recombinant

[−2]proPSA−C_κ or [−5/−7]proPSA−C_κ protein, respectively. To select binders, phage ELISA was performed using microtiter plates coated with peptide−BSA and recombinant protein as described previously (89).

9. Overexpression and purification of the antibodies for proPSAs as scFv−hFc fusion protein

From a phagemid DNAs encoding scFvs reactive to [−2]proPSA or [−5/−7]proPSA, the gene encoding scFv were prepared by digestion with SfiI restriction enzyme, 1% agarose gel electrophoresis, and DNA extraction. The gene was ligated into a pCEP4 expression vector modified to contain the human immunoglobulin Fc domain (hFc) using T4 DNA ligase (90). HEK 293F cells were transfected with the vector as described previously (81). After 5 days, overexpressed scFvs−hFc were purified from the culture supernatant by affinity chromatography using Protein A agarose beads (Repligen Corp., MA, USA) according to the manufacturer's instructions.

10. Enzyme−linked immunosorbent assay (ELISA)

The each well of the microtiter plate (Corning Costar Corp., MA, USA) was incubated with 100 ng of recombinant protein or peptide-BSA conjugates in sodium bicarbonate buffer (pH 8.6) overnight at 4 ℃. After blocking with 3% BSA (Millipore) in PBS for 1 h at 37 ℃, scFvs-hFc (2pro6P-hFc and 7pro13R-hFc) diluted in 50 ul of blocking buffer to a final concentration of 5 μg/ml were applied to each well and incubated for 1 h at 37 ℃. After washing with 0.05% Tween-20 in PBS (PBST), the samples were incubated with 1:5,000 diluted anti-human Fc-HRP in blocking buffer at 37 ℃ for 1 h. The plate was washed again and 50 μL of 2,2-azino-bis (3-ethylbenzothiazoline-6-sulphonic acid) (ABTS) substrate solution (AMRESCO, OH, USA) was added into each well. The absorbance of each well was measured at 405 nm using Labsystems Multiskan Ascent microplate reader (ThermoFisher Scientific). All the experiments were performed in triplicate.

RESULTS

Construction of expression vectors and expression of recombinant PSAs

I constructed a vector expressing a gene encoding the leader peptide of PSA (MGWSCIILFLVATATG) followed by [−2]proPSA (SRIVGGWECEKHSQ... ANP) and the human kappa constant (C_κ) domain using a mammalian expression vector. I also cloned the [−7]proPSA (APLILSRIVGGWECEKHSQ.... ANP) and PSA (IVGGWECEKHSQ.... ANP) genes into the same expression vector in place of [−2]proPSA (Figure 3A). HEK 293F cells were transfected with these expression vectors and then the culture supernatant was harvested and subjected to a purification process using KappaSelect resin reactive to the human C_κ domain. The purified proteins were resolved by SDS−PAGE and visualized by Coomassie Blue staining (Figure 3B). No other visible bands were observed except the 40 kDa band expected for the fusion proteins. To confirm the identity of the purified proteins, we performed immunoblot analysis using two commercially available antibodies; rabbit antibodies against PSA (D6B1 and D11E1) and anti−human C_κ antibody conjugated to horseradish peroxidase (HRP). Recombinant [−2]proPSA

protein, as well as the other recombinant proteins, reacted with these antibodies(Figure 3 C).

N-terminal sequencing of recombinant PSAs

For determination of residues 1-5 from N-terminus of the recombinant proteins, the proteins were analyzed by Edman degradation as described previously (91). In Edman cycles, the N-terminal amino acid in organic-based Edman reagent is converted to phenylthiohydantoin amino acid (PTH-amino acid) derivatives. The recombinant proteins generated using the expression vectors encoding [-2]proPSA-C_{κ}, [-7]proPSA-C_{κ}, and PSA-C_{κ} showed an N-terminal sequence of SRIVG with 95% purity, a mixture of LILSR and APLIL at a ratio of 7:5, and WEXEK, respectively (Figure 4). Among them, PTH-cysteine exhibited a unique property that was not detected at 269 nm, which was repeated previously (92). Therefore, the third residue in the PSA-C_{κ} fusion protein was determined to be cysteine. In Edman cycles, a carry-over (sequence lag) effect could occur in which the signal from a previous PTH-amino acid is transferred to a subsequent cycle (92) due to incomplete coupling and cleavage of the N-terminal residue. In

this study, peaks indicating glutamic acid (E) were observed at the third and fifth residue positions of the recombinant PSA-C_κ fusion protein; these were considered as carry-over. In summary, the expression vectors encoding [-2]proPSA, [-7]proPSA, and PSA generated [-2]proPSA-C_κ with 95% purity, a mixture of [-5/-7]proPSA-C_κ, and [+4]PSA-C_κ, respectively.

LC-MS/MS of recombinant PSAs

To measure an exact molecular weight, recombinant proteins were analyzed by LC-MS/MS. In the LC-MS/MS, mass to charge ratios (m/z) of [-2]proPSA-C_κ and [+4]PSA-C_κ were in the range of 400097-40770 m/z. The molecular mass of [-5/-7]proPSA-C_κ was in the range of 40664-41266 m/z. The peaks with the strongest intensity of [-2]proPSA-C_κ, [-5/-7]proPSA-C_κ and [+4]PSA-C_κ were represented at 40666 m/z, 41098 m/z and 400096 m/z, respectively (Figure 5). The molecular masses were higher than the expected value which were 38506.29 Da, 39013.63 Da and 37936.96 Da for [-2]proPSA-C_κ, [-5/-7]proPSA-C_κ and [+4]PSA-C_κ, respectively.

The differences in the molecular mass than the expected value might be caused by post-translational modifications (PTMs) such as glycosylation, acetylation, biotinylation and phosphorylation which were frequently observed in the recombinant proteins (93). Among the PTMs, glycosylation of proteins expressed in mammalian cells was common and as the glycosylation of PSA was studied already (82), it was assumed that glycosylation in [-2]proPSA-C_κ, [-5/-7]proPSA-C_κ and [+4]PSA-C_κ is responsible for increase in the molecular mass. The variations of molecular mass about 500 Da in recombinant proteins might be caused by glycosylation patterns (93) or chemical modifications such as methylation and phosphorylation in amino aicds (94).

Also, sequences of the recombinant proteins were analyzed by LC-MS/MS and sequencing resultes were matched to the expected sequences encoding [-2]proPSA-C_κ, [-5/-7]proPSA-C_κ and [+4]PSA-C_κ.

SEC-HPLC of recombinant PSAs

To validate protein properties such as aggregation, monomeric or oligomeric form and stability, SEC-HPLC under the native

condition was carried out. SEC-HPLC is a tool for analyzing percentage of small protein aggregates which exist in solution but is invisible and insoluble (95). In the SEC-HPLC, [-2]proPSA-C_κ, [-5/-7]proPSA-C_κ and [+4]PSA-C_κ showed a single peak without multiple peaks of protein aggregates (Figure 6). As peaks of recombinant proteins were discovered singly and lacated nearby peak 5 with molecular weight of 44 kDa, it was proved that [-2]proPSA-C_κ, [-5/-7]proPSA-C_κ and [+4]PSA-C_κ existed as a monomer with molecular weight about 40 kDa.

Protein stability was tested by repetitive freezing and thawing process. [-2]proPSA-C_κ, [-5/-7]proPSA-C_κ and [+4]PSA-C_κ underwent 1, 5 and 10 times of freezing and thawing individually and the recombinant proteins were analyzed by SEC-HPLC. From the SEC-HPLC, the recombinant proteins showed a single peak nearby peak 5 with molecular weight of 44 kDa regardless of the number of freezing and thawing process (Figure 7). Hence, all the recombinant proteins were resistant in generating protein aggregates even after experiencing 10 times of freezing and thawing process. In summury, [-2]proPSA-C_κ, [-5/-

7]proPSA−C_κ and [+4]PSA−C_κ generated in developed expression and purification system were very stable and existed as a monomer without protein aggregates.

Generation and characterization of anti−proPSA antibody

To geenerate polyclonal antibodies for proPSAs, Three chickens were immunized with the peptide−KLH and peptide−OVA conjugates, alternatively. Then a phage display of a combinatorial scFv library was generated using cDNA prepared from bone marrow, spleen, and bursa of Fabricius of immunized chickens. 2pro6P and 7pro13R antibody were selected using phage display technique.

The 2pro6P was expressed as scFv−hFc fusion protein reacted very specifically to the 2pro−BSA and [−2]proPSA−C_κ fusion proteins without crossreacting to other controls in ELISA (Figure 8A) and immunoblot analysis (Figure 9). Critical residue for antigen−antibody binding of 2pro6P is considered as of the S residue at the N−terminus in [−2]proPSA because [−5]proPSA and [−7]proPSA contain the entire amino acid sequence of [−2]proPSA. The 7pro13R was also expressed as scFv−hFc fusion protein bound to the 7pro−BSA, 5pro−BSA

and [−5/−7]proPSA−C_{κ} fusion proteins without crossreacting to other controls in ELISA. Epitope of 7pro13R is considered as of the L residue at the N−terminus in [−5/−7]proPSA because [−5]proPSA and [−7]proPSA contain leucine residue in common (Figure 8B).

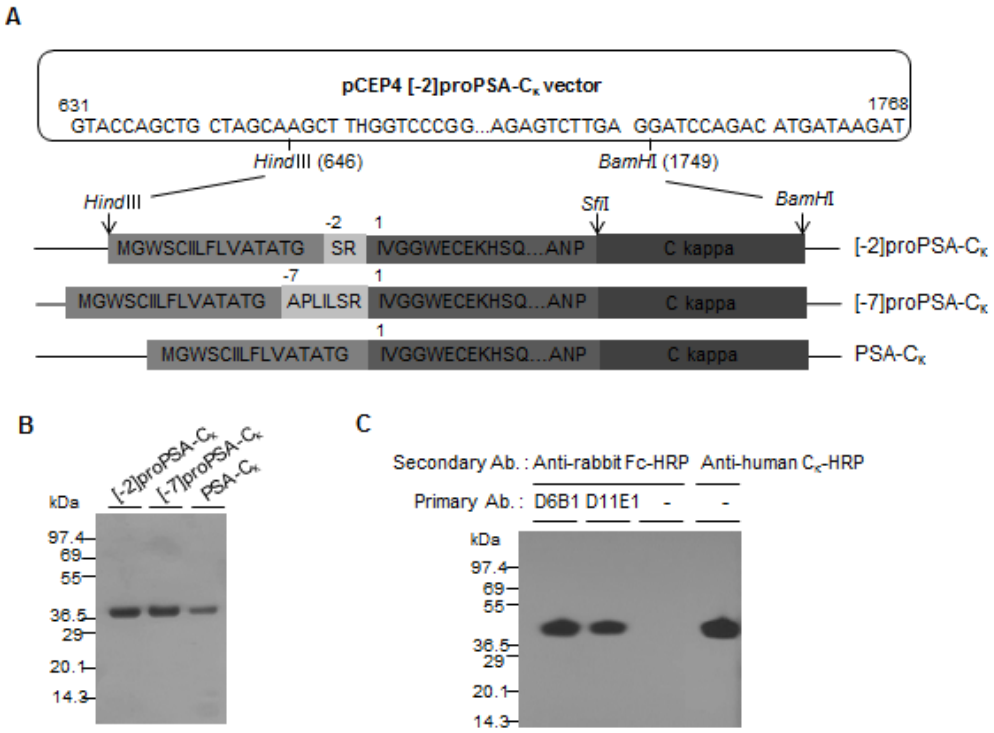

Figure 3. Overexpression and purification of recombinant [−2], [−7]proPSA, and PSA. (A) Schematic diagram of recombinant PSA expression vectors. The gene encoding the leader peptide of PSA followed by [−2]proPSA, [−7]proPSA, or PSA and the human kappa constant (C_κ) domain were cloned into mammalian expression vector pCEP4. (B) Recombinant proteins were overexpressed in HEK 293F cells and purified by affinity chromatography. Purified recombinant proteins were subjected to 4−12% SDS−PAGE and visualized by Coomassie Blue staining. (C) Recombinant [−2]proPSA−C_κ protein was subjected to 4−12% SDS−PAGE, transferred to nitrocellulose

membrane, and then incubated with two commercially available rabbit anti-PSA antibodies, D6B1 and D11B1, followed by HRP-conjugated anti-rabbit IgG (Fc-specific) antibody (anti-rabbit Fc-HRP). The membrane was also probed with anti-rabbit Fc-HRP or HRP-conjugated anti-human C_{κ} antibody only.

A

Blank (Y axis : -2~42mV)

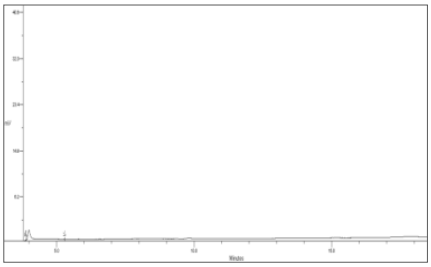

The 1st residue

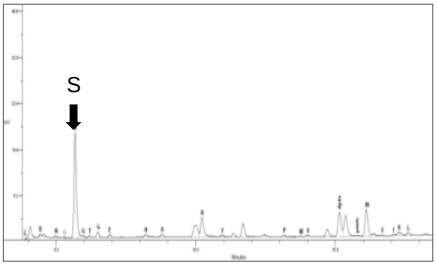

The 2nd residue

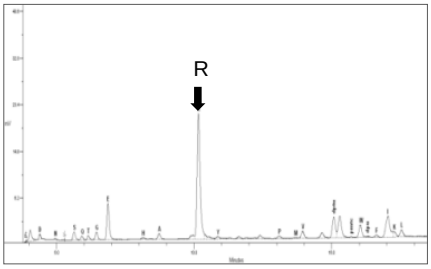

The 3rd residue

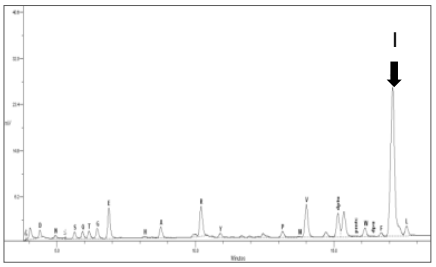

The 4th residue

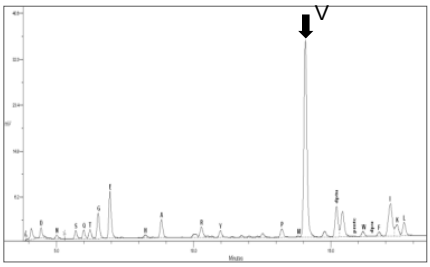

The 5th residue

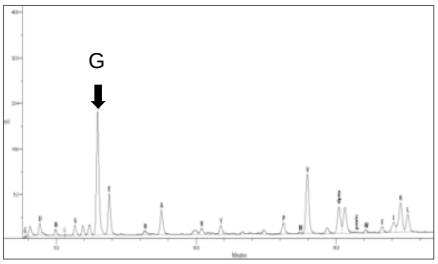

B

Blank (Y axis : -2~25mV)

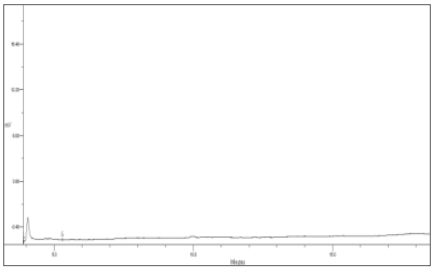

The 1st residue

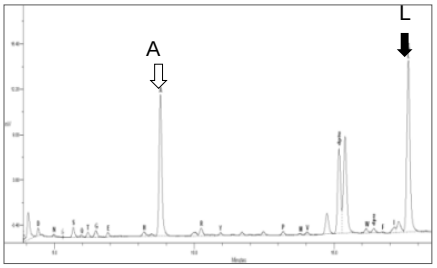

The 2nd residue

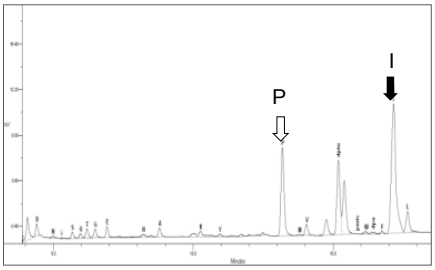

The 3rd residue

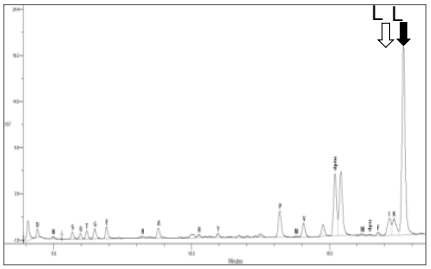

The 4th residue

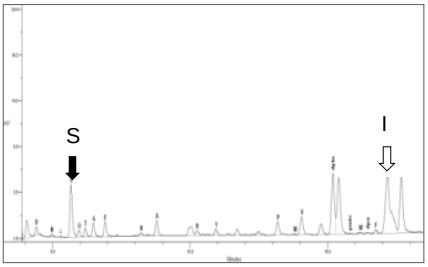

The 5th residue

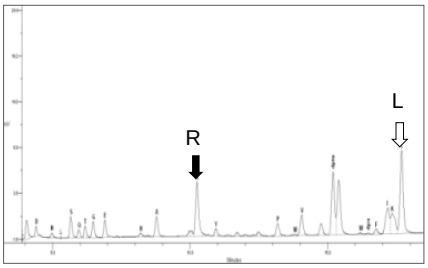

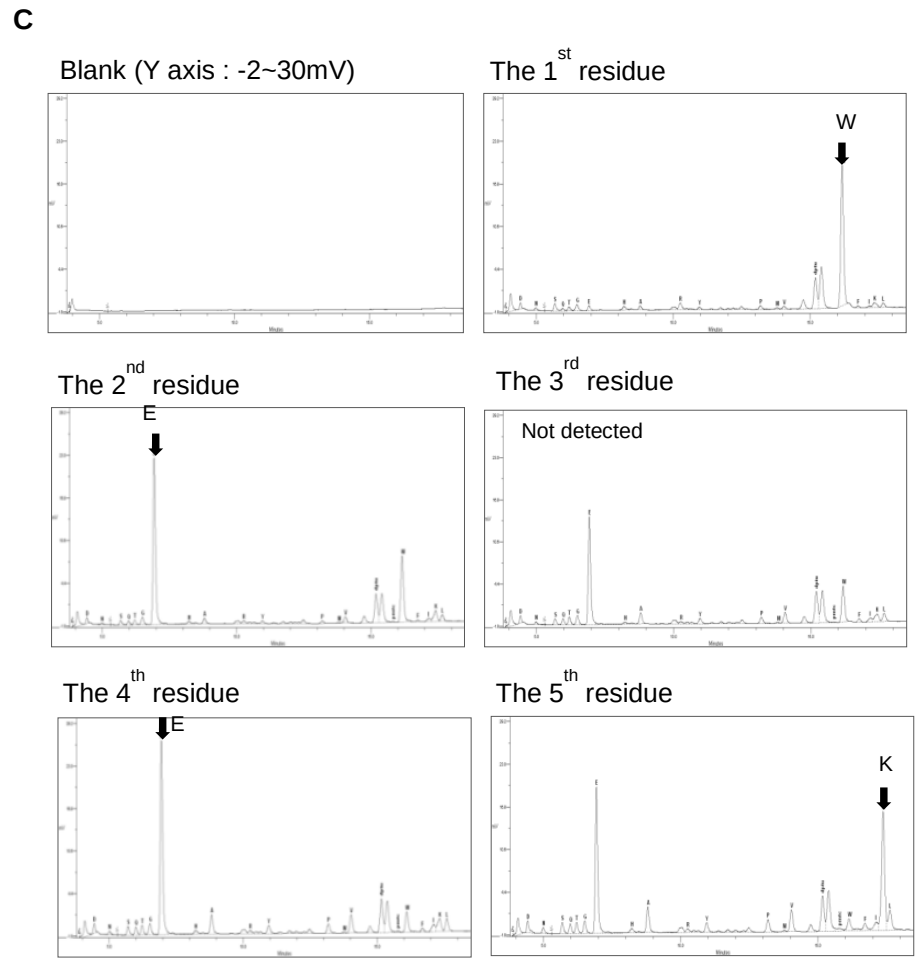

Figure 4. N-terminal sequencing of recombinant proteins. High pressure liquid chromatography was performed after Edman degradation of the recombinant proteins purified from the culture supernatant of HEK 293F cells transfected with expression vector encoding (A) [-2]proPSA-C_{κ}, (B) [-7]proPSA-C_{κ}, and (C) PSA-C_{κ}. Black arrows indicate major amino acids and white arrows indicate minor amino acids at each position.

A

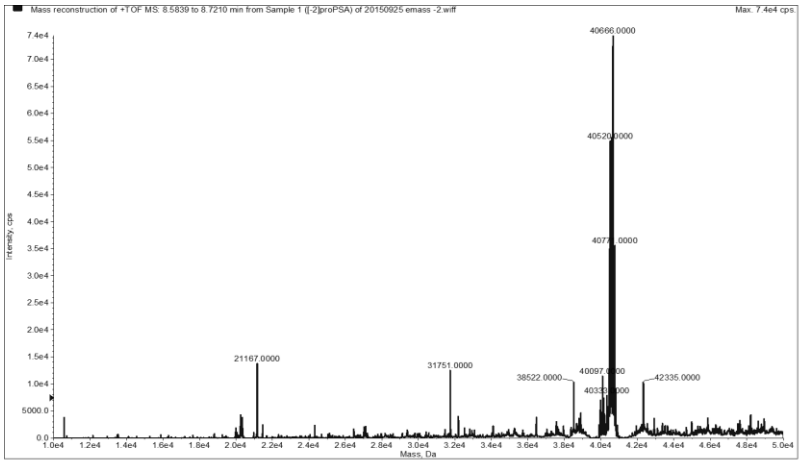
Mass reconstruction of +TOF MS: 8.5839 to 8.7210 min from Sample 1 ([-2]proPSA) of 20150925 emass -2.wiff
Max. 7.4e4 cps.
Intensity, cps
Mass, Da
40666.0000
40520.0000
21167.0000
31751.0000
38522.0000
42335.0000

B

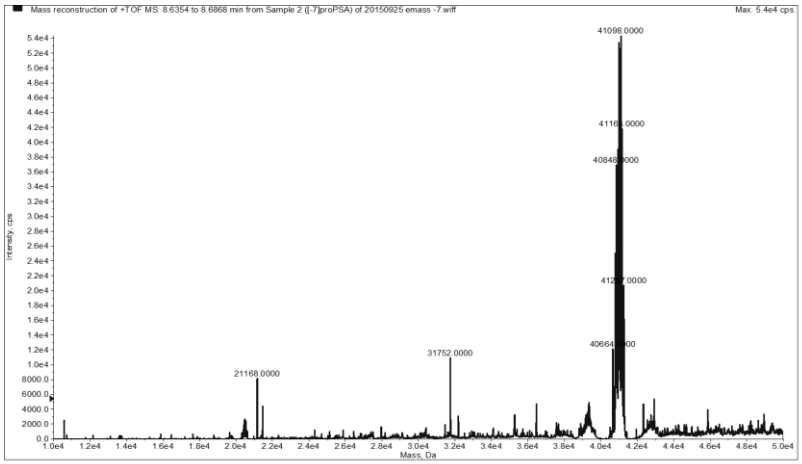
Mass reconstruction of +TOF MS: 8.6354 to 8.6868 min from Sample 2 ([-7]proPSA) of 20150925 emass -7.wiff
Max. 5.4e4 cps.
Intensity, cps
Mass, Da
41098.0000
41168.0000
40848.0000
40664.0000
21168.0000
31752.0000

C

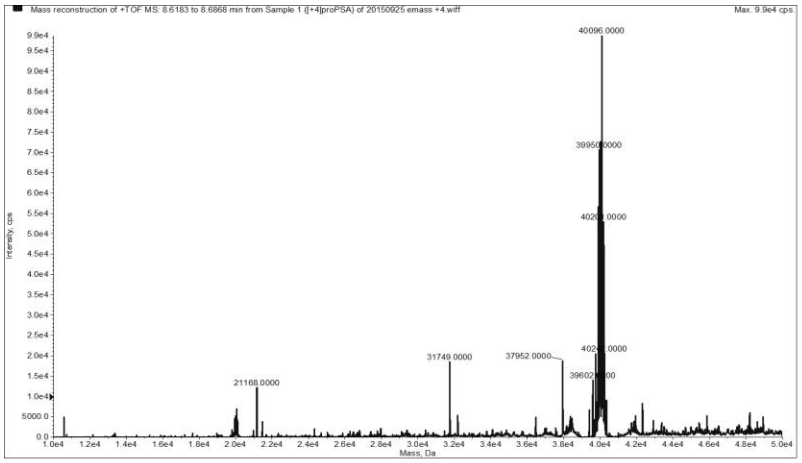

Figure 5. LC-MS/MS of recombinant proteins. LC-MS/MS was performed to determinea an exact molecular weight of recombinant proteins purified from the culture supernatant of HEK 293F cells transfected with expression vector encoding (A) [-2]proPSA-C_{κ}, (B) [-5/-7]proPSA-C_{κ}, and (C) [+4]PSA-C_{κ}.

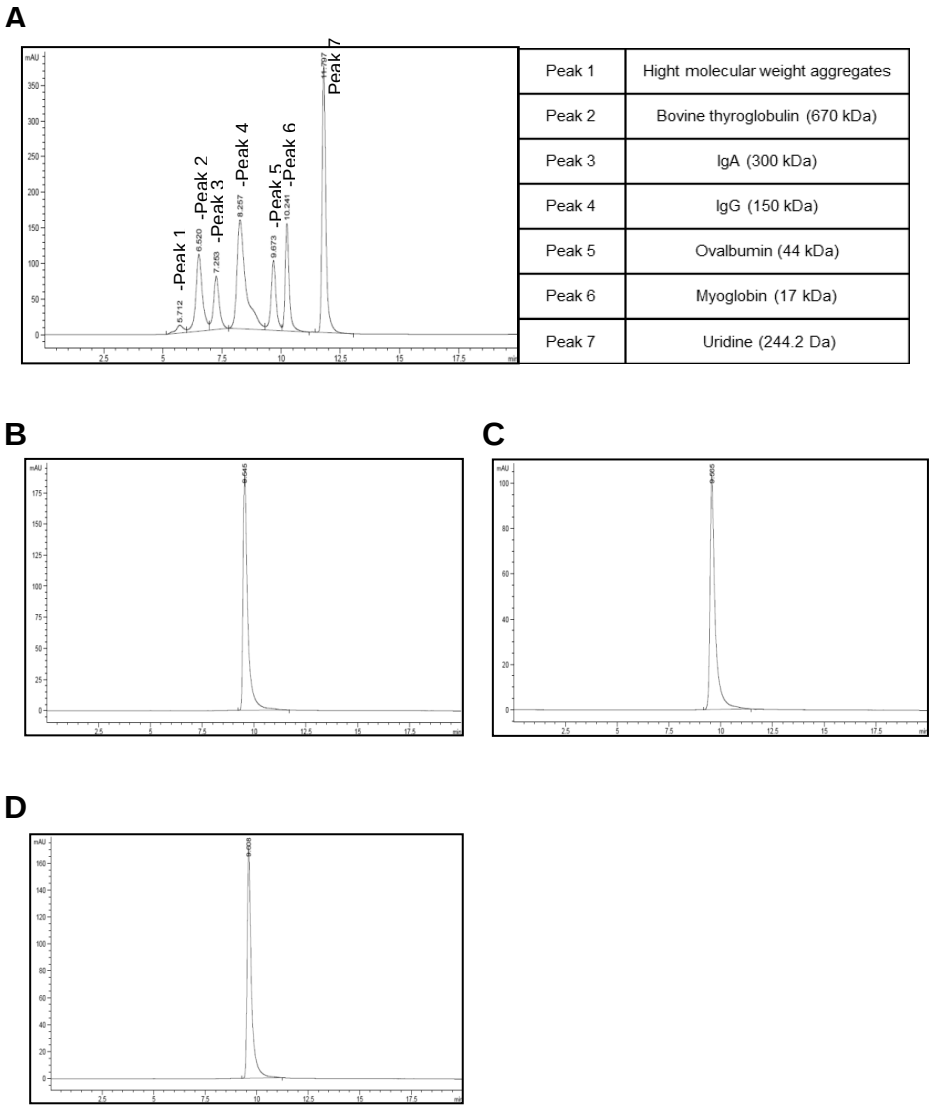

Peak 1	Hight molecular weight aggregates
Peak 2	Bovine thyroglobulin (670 kDa)
Peak 3	IgA (300 kDa)
Peak 4	IgG (150 kDa)
Peak 5	Ovalbumin (44 kDa)
Peak 6	Myoglobin (17 kDa)
Peak 7	Uridine (244.2 Da)

Figure 6. SEC-HPLC of recombinant proteins. To validate protein properties such as aggregatation and formet, recombinant proteins were analyzed by SEC-HPLC. (A) The standards used were bovine thyroglobulin, IgA, IgG, ovalbumin, myoglobin and uridine. (B) [-2]proPSA-C_{κ}, (C) [-5/-7]proPSA-C_{κ}, and (D) [+4]PSA-C_{κ}.

A

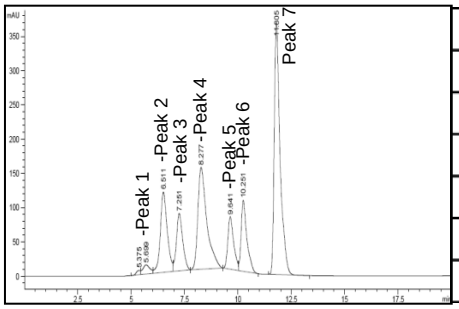

Peak 1	Hight molecular weight aggregates
Peak 2	Bovine thyroglobulin (670 kDa)
Peak 3	IgA (300 kDa)
Peak 4	IgG (150 kDa)
Peak 5	Ovalbumin (44 kDa)
Peak 6	Myoglobin (17 kDa)
Peak 7	Uridine (244.2 Da)

B

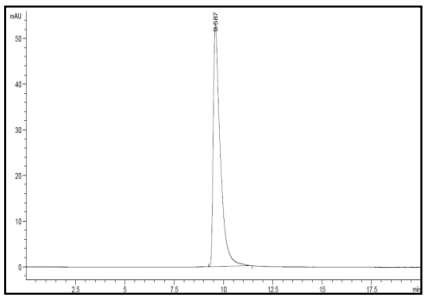

C

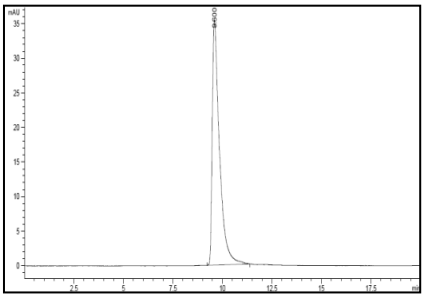

D

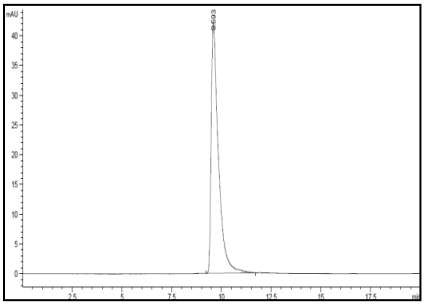

E

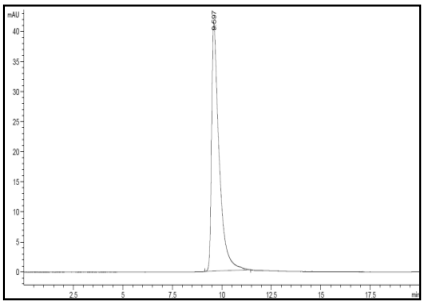

F

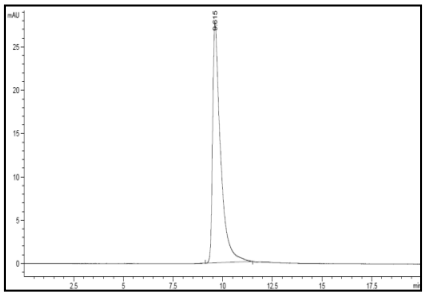

G

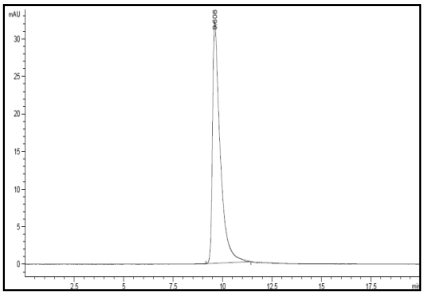

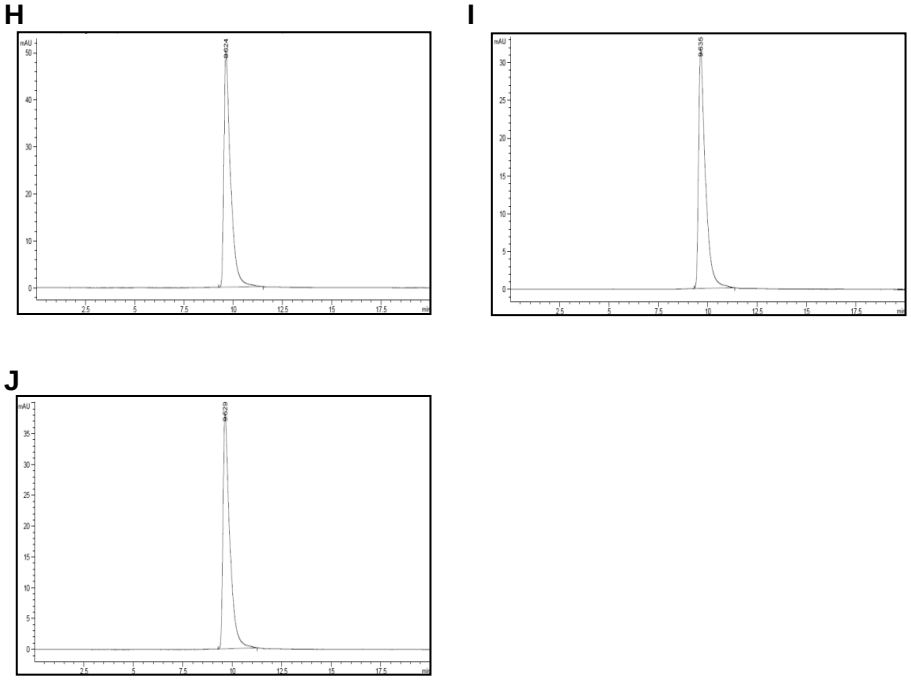

Figure 7. Stability test of recombinant proteins. Recombinant proteins were underwent 1, 5 and 10 times of freezing and thawing process individually and the recombinant proteins were analyzed by SEC-HPLC. (A) The standards used were bovine thyroglobulin, IgA, IgG, ovalbumin, myoglobin and uridine. (B) [-2]proPSA-C_{κ} with 1 time of freezing and thawing process, (C) [-2]proPSA-C_{κ} with 5 times of freezing and thawing process, (D) [-2]proPSA-C_{κ} with 10 times of freezing and thawing process, (E) [-5/-7]proPSA-C_{κ} with 1 time of freezing and thawing process, (F) [-5/-7]proPSA-C_{κ} with 5 times of freezing and thawing process, (G) [-5/-7]proPSA-C_{κ} with 10 times of freezing and thawing process, (H) [+4]PSA-

C_K with 1 time of freezing and thawing process, (I) [+4]PSA-C_K with 5 times of freezing and thawing process, (J) [+4]PSA-C_K with 10 times of freezing and thawing process.

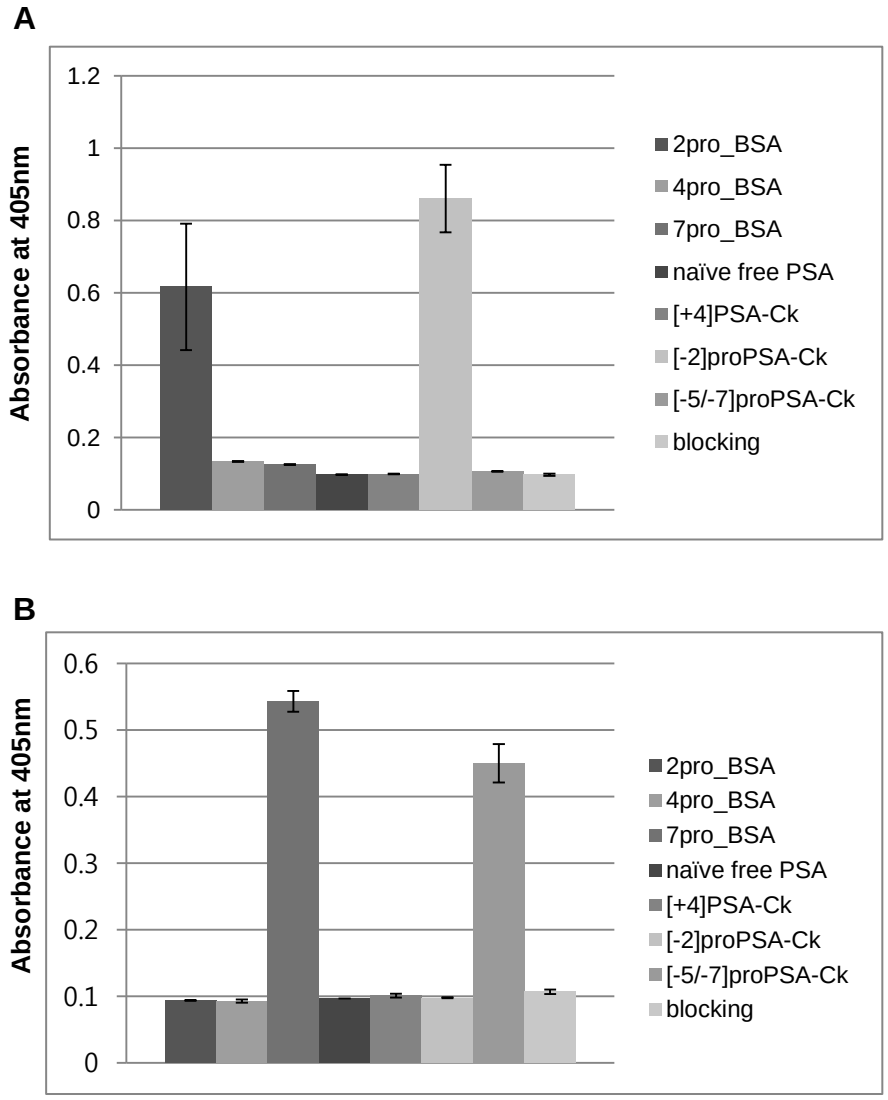

Figure 8. Epitope mapping of antibodies against [−2]proPSA and [−5/−7]proPSA protein. (A) Various peptide−BSA conjugates, naïve PSA and recombinant proteins were coated on microtiter plate The microtiter plate was incubated with 2pro6P−hFc for [−2]proPSA, then probed with HRP−conjugated anti−human Fc antibody (anti−human Fc−HRP). Absrobance was measured at

405 nm (B) Various antigens such as proteins and peptide conjugates were coated on microtiter plate The microtiter plate was incubated with 7pro13R-hFc for [-5/-7]proPSA, then probed with HRP-conjugated anti-human Fc antibody.

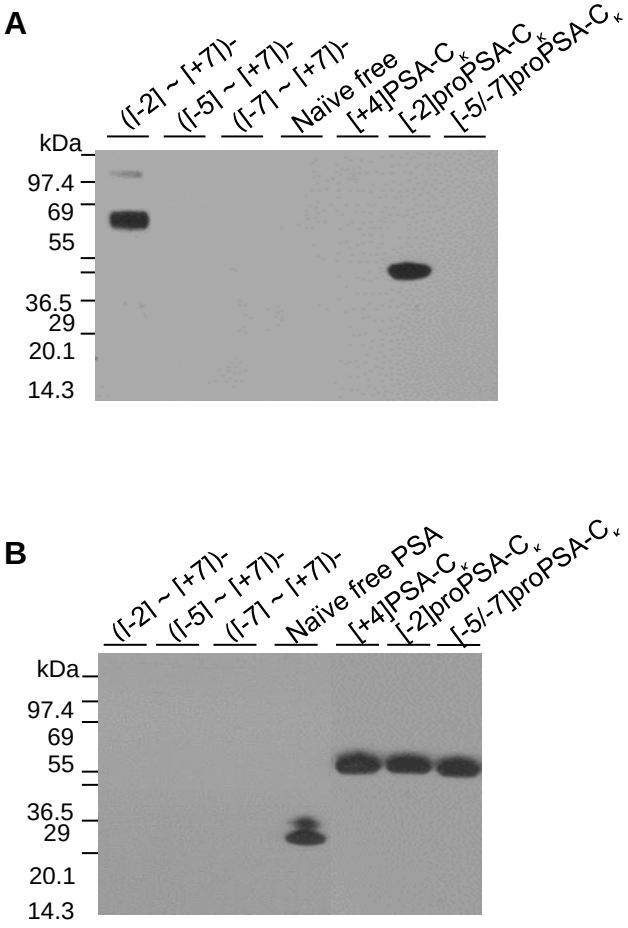

Figure 9. The specificity test of 2pro6P antibody. (A)Various peptide-BSA conjugates and recombinant proteins were subjected to 4-12% SDS-PAGE and transferred onto nitrocellulose membrane. The membrane was incubated with 2pro6P scFv-hFc, then probed with HRP-conjugated anti-human Fc antibody (anti-human Fc-HRP). (B) Various peptide-BSA conjugates and recombinant proteins were subjected to 4-12% SDS-PAGE and then transferred onto

nitrocellulose membrane. The membrane was incubated with D6B1 antibody and probed with anti-rabbit Fc-HRP.

DISCUSSION

PSA or kallikrein-related peptidase 3 is encoded by a single gene (KLK3) located at chromosome 19q13.41. During the post-translational modification process, the N-terminal leader peptide is removed. Studies have shown that [-7], [-5], [-4], and [-2]proPSA could be generated during this process. Of these four proPSAs, [-2]proPSA is the most extensively studied biomarker (96, 97). To measure the serum [-2]proPSA level by ELISA, the [-2]proPSA standard and specific antibody are essential. Since the amount of [-2]proPSA in serum or semen is quite low (1). it is impractical to purify it from biological fluid. Until now the whole PSA gene is cloned into expression vector and [-2]proPSA generated in minor fraction is purified using high-performance hydrophobic interaction chromatography (98). In this study, I constructed an expression vector with a sequence composed of the PSA leader peptide and [-2]proPSA fused with human C_{κ} domain immediately following the C-terminus of PSA. Edman degradation analysis was revealed that [-2]proPSA is the major form of the recombinant protein. The enzyme responsible for digesting the final amino acid of the leader peptide (G) and

the first amino acid of [−2]proPSA (S) could be either hK2 or prostin (99). In LC−MS/MS, molecular weights of [−2]proPSA, [−5/−7]proPSA protein were confirmed to be 40.666 kDa and 41.098 kDa, respectively. Moreover, it was validated by SEC−HPLC that recombinant proteins generated in developed expression and purification system was stable and existed as a monomer without protein aggregates.

The 7pro13R and 2pro6P antibody were produced and isolated following chicken immunization with peptide−KLH and peptide−OVA, alternatively. The 7pro13R−hFc bound to the 7pro−BSA, 5pro−BSA and [−5/−7]proPSA−C_{κ} fusion proteins without crossreacting to naïve free PSA, [+4PSA and [−2]proPSA in ELISA. Epitope of 7pro13R is considered as of the L residue at the N−terminus in [−5/−7]proPSA because [−5]proPSA and [−7]proPSA contain leucine residue in common. The 2pro6P preferentially bound to [−2]proPSA but not to naïve free PSA, [+4]PSA, [−5] proPSA, or [−7] proPSA. Since [−5]proPSA and [−7]proPSA contain the entire amino acid sequence of [−2]proPSA, the position of the S residue at the N−terminus is considered to be critical for antibody binding. Moreover, these antibodies reacted to the native form of [−

2]proPSA-C_κ coated directly onto the plate or captured by an anti-PSA antibody. These data suggest that the N-terminus of [-2]proPSA-C_κ is exposed on the outside of the protein in its native form. Because this antibody reacted to the denatured form of [-2]proPSA in immunoblot analysis, it is clear that the N-terminus of [-2]proPSA is also exposed after denaturation. This observation raised the possibility that this antibody could be used to visualize proPSAs in immunohistochemical analysis.

I also attempted to use developed antibodies to immunoprecipitate proPSAs from patient sera, but the experiment was not successful. Additional investigation to increase the affinity of the antibody or to better prepare the sample may be necessary to immunoprecipitate proPSAs from biological samples. As there is already a commercially available assay kit for determining the concentration of proPSAs (100), I think that immuno-affinity purification of proPSAs from sera could be achievable after affinity maturation of the antibody.

CHAPTER 2

Antibody and Raman imaging

INTRODUCTION

SWNT as a Nanomaterial

Nanomaterials have been widely used in various applications ranging from biomedicine (101-103) to electronics (104-106). There is various nanomaterials such as quantum dots, nanowires, gold nanoparticles, nano-Photonics, magnetic nanostructures and new format nanomaterials under developeing

Nanomaterials have the potential to be applied to bioimaging since nanonaterials emit higher and longer fluorescence than conventional organic probes. They have been expected to be applied in biomedical fields such as biomaterials, immunoassay, diagnostics, and even in therapeutic (107). As the biomedical probes, nanomaterials were required to be conjugated with biomolecules such as antibodies, peptides and DNAs to detect for their specific target molecules (108-111) by chemical conjugation processes.

Several conjugation steps, however, significantly affects the binding efficacy between nanomaterial bioconjugates and target molecules. Therefore, controling density of biomolecules per nanomaterial and orientation on the nanomaterial interface were

very essential for maximizing the binding efficiency between biomedical probes and target molecules. Many studies have been reported to control the orientation and position of protein ligands on nanomaterials, including biotin-avidin affinity chemistry (112), bioorthogonal cycloaddition chemistry (113, 114), metal-affinity coordination with histidine-tagged proteins(115, 116), and scFv antibody fused with a nanoparticle-capture domain (117, 118). However, there is needs for development of advanced conjugation approaches that can lead to enhancement of the effective binding between nanomaterial and target molecules by adjusting the molecular arrangement.

Among nanomaterials, Single-walled carbon nanotube (SWNT) kind of Carbon nanotubes (CNTs), is allotropes of carbon with a nanostructure. SWNT have a 1 nanometer diameter, with a tube length that can be up to 28 million times longer than other materials and structure of a SWNT is cylinder. Depending on their structure the SWNTs are named as zigzag, armchair, graphene nanoribbon or chiral. SWNT is the most likely candidate for miniaturizing electronics beyond the micro electromechanical scale currently used in electronics. SWNT is

ideal nanomaterial as a biosensor and imaging platform because it exhibits near-infrared (NIR) photoluminescence (119) without photobleaching threshold and show strong resonance Raman signal (120, 121). As these outstanding properties of SWNT, it have been applied in the detection of target molecules (122) and imaging for tissue (101) and tumor (106).

Bispecific tandem antibody

Bispecific tandem antibody is composed two single-chain variable fragment (scFv) and human constant region. Bispecific antibodies bound to target molecules and cotinine, a hapten, simultaneously (Figure 10). Cotinine is a small size molecule and has many advantages to be used as a hapten. As a metabolite of nicotinine, cotinine is very safe and stable in our body (123). Also, as described above, cotinine is non-immunogenic in our body. *Trans*-4-cotininecarboxylic acid is easy to induce chemical reaction by its functional group, as well (124). Because anti-cotinine scFv antibody in bispecific antibody binds to SWNT coated cotinine with hight affinity, scFv antibody being another component of bispecific antibody is exposed freely. It might give a direction or orientation of the

bispecific antibody on SWNT surface.

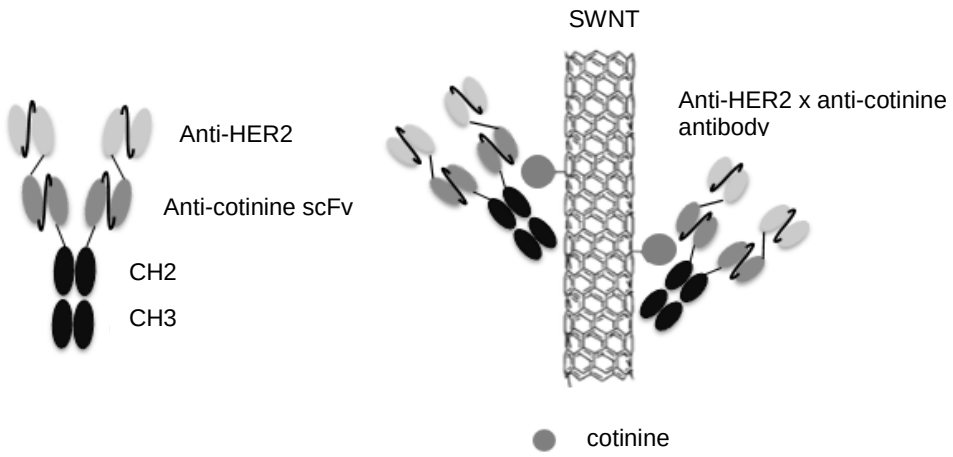

Figure 10. The construction of bispeicific antibody and SNA. (A) The bispecific antibody is composed of anti-HER2 scFv, anti-cotinine scFv and human Fc domain. (B) Diagram of SNA. The SNA was consisted of SWNT chemically synthezied with cotinine and anti-HER2 × cotinine antibody.

MATERIAL AND METHODS

1. Construction and expression of bispecific antibodies.

Bispecific tandem antibody composed of two scFv antibodies and the hinge region of human IgG1 and the CH2-CH3 domains. Two Sfi I restriction enzyme sites was used anti-HER2 or anti-PSA scFv insertion, Age I (Invitrogen, Grand Island, NY) and Not I (Invitrogen) restriction enzyme sites for anti-cotinine scFv insertion. Sequence confirmed clone was transfected to 293F cells using 25 kDa linear polyethylenimine according to previous reports, 2.5 μg/mL plasmid DNA and 5 μg/mL polyethylenimine mixed in prewarmed 150 mM NaCl solution. After 15 min incubation at room temperature, added 2 $\times$ 10^6 cells/mL HEK293F cells. The cells were grown in FreeStyle 293 Expression Medium for 5 days at 37 ℃ in anatmosphere containing 7% CO_2 on an orbital shaking incubator (Minitron) at 135 r.p.m. After five days, supernatant was harvested and purified using protein A bead (RepliGen, Waltham, MA) following manufacturer's instructions.

2. Binding test of expressed bispecific antibodies

The each well of the microtiter plate was incubated with 100 ng of HER2 or PSA in sodium bicarbonate buffer (pH 8.6) overnight at 4 ℃. After blocking with 3% BSA in PBS for 1 h at 37 ℃, anti-HER2 × cotinine antibody or anti-PSA × cotinine antibody diluted in 50 μL of blocking buffer to a final concentration of 5 μg/mL was applied to each well and incubated for 1 h at 37 ℃. After washing with 0.05% Tween-20 in PBS (PBST), the samples were incubated with 1: 500 diluted cotinine-HRP at 37 ℃ for 1 h. The plate was washed again and 50 μL of 1,3,5-trimethylbenzene (TMB) substrate solution was added into each well. The absorbance of each well was measured at 650 nm using Labsystems Multiskan Ascent microplate reader.

3. Synthesis of Cotinine-Modified Phenoxy Dextran

To synthesize PhO-dex, 1 g of dextran (10 kDa) was dissolved in a 1 M NaOH solution (10 mL) and 0.75 mL of 1,2-epoxy-3-phenoxypropane added (125). After stirring at 40 ℃ for 10 h, 150 mL of methanol were slowly added into the mixture to precipitate the desired product (PhO-dex). Then, mixture was washed with methanol several times and dried. To introduce the

cotinine groups to PhO-dex, Cot (0.13 or 0.4 g) was added to the PhO-dex/DMF solution (1 g of PhO-dex in 50 mL DMF) in the presence of (benzotriazol-1-yloxy)tris(dimethylamino) phosphonium hexafluorophosphate (BOP, 0.4 or 1.2 g) and 4-(dimethylamine)pyridine (DMAP, 0.1 or 0.3 g). stirring mixture at 60 ℃ for 5 h, then 500 mL of methanol was added slowly into the mixture to precipitate products (1-Cot-PhO-dex and 3-Cot-PhO-dex). The precipitated products were purified by dialysis in water using a cellulose dialysis membrane (MWCO 8 kDa) for three days and dried.

4. Synthesis of the SWNT/Bispecific Tandem Antibody Conjugates (SNAs)

Five milligrams of SWNTs (CoMoCAT) were added into a 5 mL Cot-PhO-dex aqueous solution (10 mg/mL), and then the mixture was sonicated using a probe tip sonicator (10 W) for 90 min in an ice. The SWNT dispersion was centrifuged at 15,000 g for 1.5 h, and collected the supernatant. To synthesize the SWNT with bispecific antibody, SWNT solution was first centrifuged with a centrifugal filter device (MWCO 100 kDa) to remove the free Cot-PhO-dex polymer in solution as well as

to exchange water with PBS (pH 7.4, 10 mM). After 25.08 g bispecific antibody was added into 0.956 mL of functionalized SWNT solution (0.84 mg/mL), resulting solution was gently shaken for 4 h at room temperature. Unbound antibodies were removed by centrifugation at 5,000 g using a centrifugal filter device (MWCO 300 kDa). The synthesized SNA was analyzed by PL, Raman spectroscopy (Alpha 300 R+, WITec, Germany).

5. Measurement of the affinity of SNA against HER2

After injecting the PBS solution containing Tween-20 (0.005 vol%) into a sensor chip in a BIAcore instrument for 10 min, an EDC/NHS solution (0.6 M of EDC and 0.2 M of NHS) was injected into the CM5 chip at 10 μL/min for 5 min to activate the carboxyl groups on the chip surface. After the chip was washed with PBS for 5 min to remove an excess of reagents, a 90 μL of target molecule (HER2-Fc, 75 μg/mL) was injected into the chip until the response signal reached 24,000 RU. After washing the chip with the PBS solution containing Tween-20 (0.005 vol%), 50 μL of ethanolamine (0.5 M) were injected to deactivate the carboxyl-NHS ester. After the chip bearing HER2-Fc was washed with a running buffer (PBS), 200 μL of

SNA (100 to 800 μg/mL) were injected at 10 μL/min until a saturated response was observed. Then, the running buffer flowed over the chip for 10 min. After each cycle of the experiment, the sensor chip was regenerated by the injection of a glycine/HCl solution (10 mM, pH 2.0) for 6 min. The measurement of the effective binding affinity of the SWNT bioconjugate which was a product of EDC coupling with bispecific antibody and SWNT was also carried out in the same way.

6. Raman imaging of cancer cells with SNA

The SNA was applied to the detection and imaging of HER2-overexpressing cancer cells. The receptor tyrosine kinase HER2 is overexpressed in various cancer tissues including breast and ovarian cancer (126) making it an important biomarker for the diagnosis of cancers. The SK-BR-3 breast cancer cell, which is well known to overexpress HER2 (127) was chosen as a positive cell line for the detection of HER2 on the cell surface with SNA. As a negative control cell, the MCF-7 breast cancer cell that exhibits a very low HER2 expression level was chosen. SNA (10 μg/mL) was incubated with each

cell line at 25 ℃ for 1.5 h after the cells were fixed to prevent the internalization of the SNA into the cytosol. Then, the SNA treated cells were washed with the cell medium and PBS (pH 7.4) several times, and they were imaged using a confocal microscope Raman system.

RESULTS

ELISA of bispecific antibodies

HEK 293F cells were transfected with gene either anti-HER2 x cotinine antibody or anti-PSA × cotinine antibody in pCEP4 vector and then cultured. After 5 days, supernatants were harvested and expressed proteins were purified by protein A beads reactive to the human Fc domain. To confirm binding property of the purified bispecific antibodies, ELISA was carried out. In ELISA, expressed anti-HER2 × cotinine antibody and anti-PSA × cotinine antibody were individually reactive to cotinine and target molecules, simultaneously (Figure 11).

Analysis of SWNT with bispecific antibody (SNA)

The SNA displayed strong NIR fluorescence in their excitation/emission profile. In the Raman spectroscopy (Alpha 300 R+, WITec, Germany), the relative intensity of the SNAs decreased slightly after the conjugation of bispecific antibodies to SNAs due to the charge transfer from SNAs to the redox active moieties such as tyrosine, tryptophan and histidine in the antibodies. This intensity decrease of SNAs fluorescence by

protein adsorption was also observed in the previously reported literature (116). Therefore, this decrease in fluorescence intensity indirectly suggests the successful conjugation of the tandem antibodies to the carbon nanotube. Anti-HER2 × cotinine antibody and anti-PSA × cotinine antibody showed a strong resonance of Raman peak at 1593 cm^{-1}, and 1583 cm^{-1}, respectively (Figure 12). It could be used as an optical signal for the selective detection of target molecules.

Measurement of the affinity of SNAs against HER2

To examine the effect of antibody orientation and density on the effective binding affinity of the SNA against HER2, we measured the binding kinetics by BIAcore assay. The target molecule, HER2, was immobilized on the sensor chip surface as previously reported (128), which resulted in the HER2 density of 250 fmol/mm(129). To determine the binding rate constants of the SNAs for HER2, the concentrations of SNA and the SWNT bioconjugate were varied from 100 to 800 μg/mL. The response values for SNA and the SWNT bioconjugate were increased with incresement of the injection concentrations. It is indicating that the association between the SNA and HER2

occurred on the chip surface. After the injection of a running buffer into the chip, the dissociation value was also measured. Then, the result of sensorgrams were fitted by a Langmuir binding model to obtain the binding rate constants as well as the equilibrium dissociation constants of the SNA and the SWNT bioconjugate. SNA containing the orientation controlled antibody showed a much lower equilibrium dissociation constant (K_D) of 4.73×10^{-9} M than that of the SWNT bioconjugate with antibody attached randomly which represented a K_D of 1.54×10^{-6} M (Figure 13). This lower equilibrium dissociation constant of SNA indicates that its effective binding affinity against HER2 is three orders of magnitude higher than that of the SWNT bioconjugate. This result suggests that an increase in the density of an orientation-controlled tandem antibody on the SWNT surface allows further enhancement of the effective binding affinity of an SNA to the target. This affinity enhancement by density control of an tandem antibody at the nanoscale might be attributed to the improved multivalency of SNA for the target (130). Therefore, SNA could be employed for the selective detection and imaging of HER2-overexpressing cancer cells.

Raman imaging of cancer cells with SNA

SNA was applied to the detection and imaging of HER2-overexpressing cancer cells using Raman signal. The receptor tyrosine kinase HER2 is overexpressed in various cancer tissues including breast and ovarian cancer(126), making it an important biomarker for the diagnosis of cancers. The SK-BR-3 breast cancer cell, which is well known as HER2 overexpression cell (127), was chosen as a positive cell line for the detection of HER2 on the cell surface with SNA. As a negative control cell, the MCF-7 breast cancer cell that exhibits a very low HER2 expression level was chosen. SNA (10 μg/mL) was incubated with each cell line at 25 ℃ for 1.5 h after the cells were fixed to prevent the internalization of the SNA into the cytosol. Then, the SNA treated cells were washed with the cell medium and PBS (pH 7.4) several times, and they were imaged using a confocal microscope Raman system. Raman signal was not detectable in the MCF-7 cell imaging with SNA by Raman. On the other hands, a strong Raman signal was clearly observed in the Raman imaging of the SK-BR-3 cells with SNA (Figure 14). In summary, SNA was able to selectively detect HER2 molecules on SK-BR-3 cells which is

the HER2-overexpressing cancer cells.

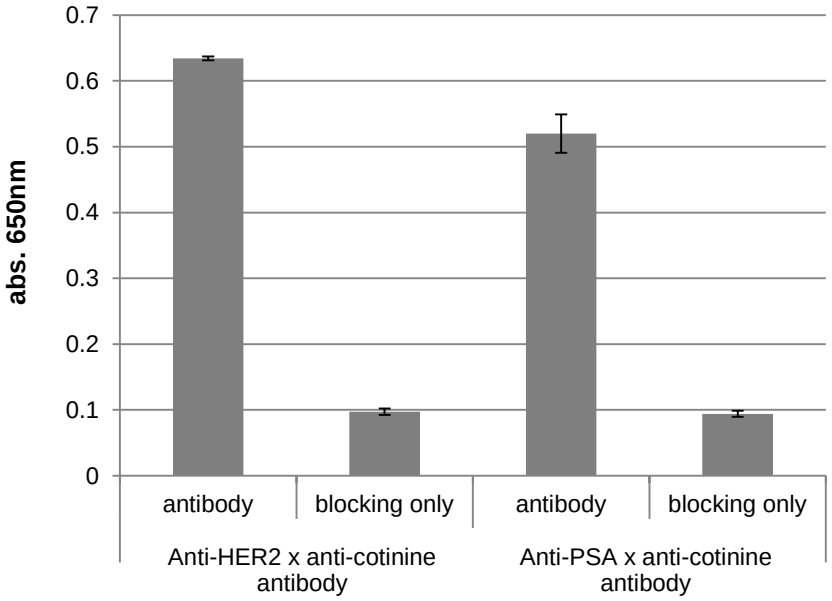

Figure 11. Binding test of bispecific antibodies. Expressed bispeicifc antibodies were incubated with HER2 or PSA antigen coated on microtiter plate. After 1h, cotinine-HRP as the 2nd antibody was added into well and incubated for 1 h, then absorbance was measured at 650nm.

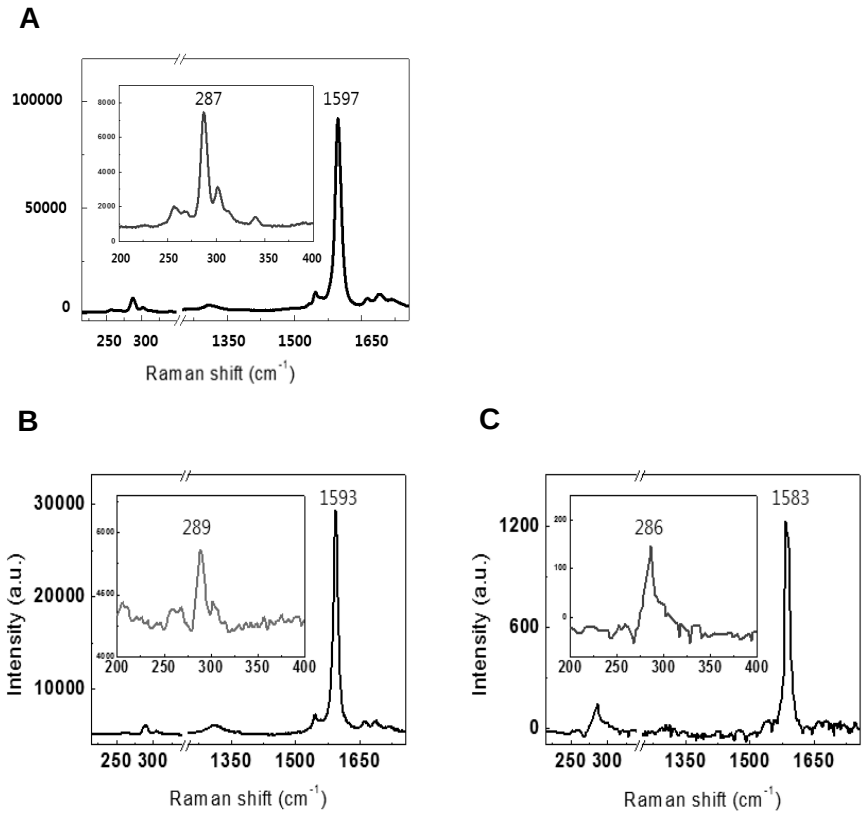

Figure 12. Raman spectroscopy of SNAs. (A) Raman spectroscopy of SWNT (B) In Raman spectroscopy, anti-HER 2 × cotinine antibody was shown a peak at 1593 cm^{-1}. (C) Raman spectroscopy, anti-PSA × cotinine antibody represented a peak wich was appeared at 1583 cm^{-1}.

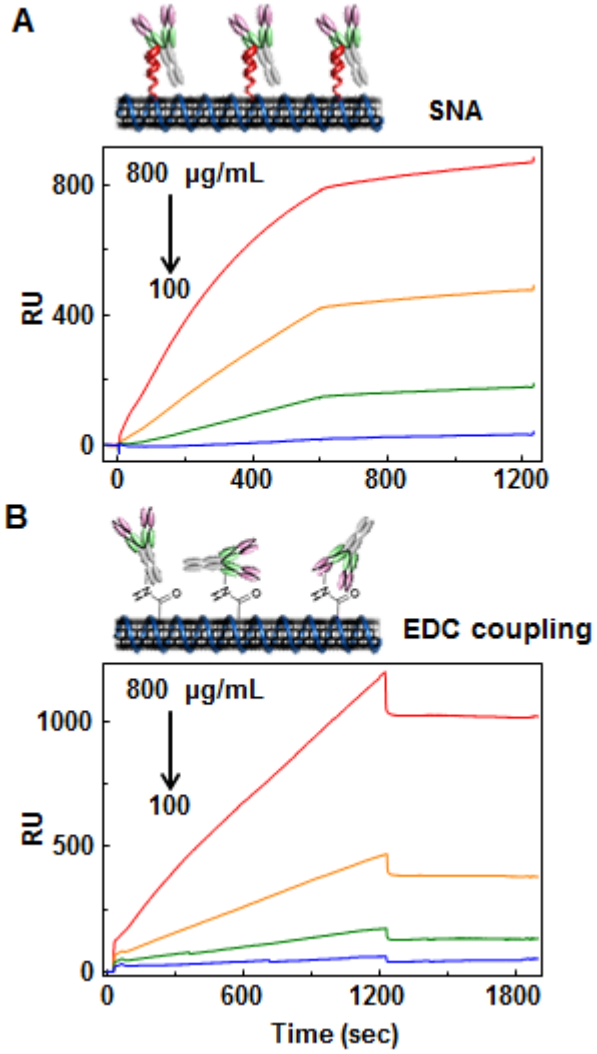

Figure 13. SPR sensorgrams for the binding of SNA and SWNT bioconjugates to HER2. (A) SPR sensorgrams of SNA (B) SPR sensorgrams of SWNT bioconjugate. The concentration of SNAs was varied from 100 to 800 μg/mL.

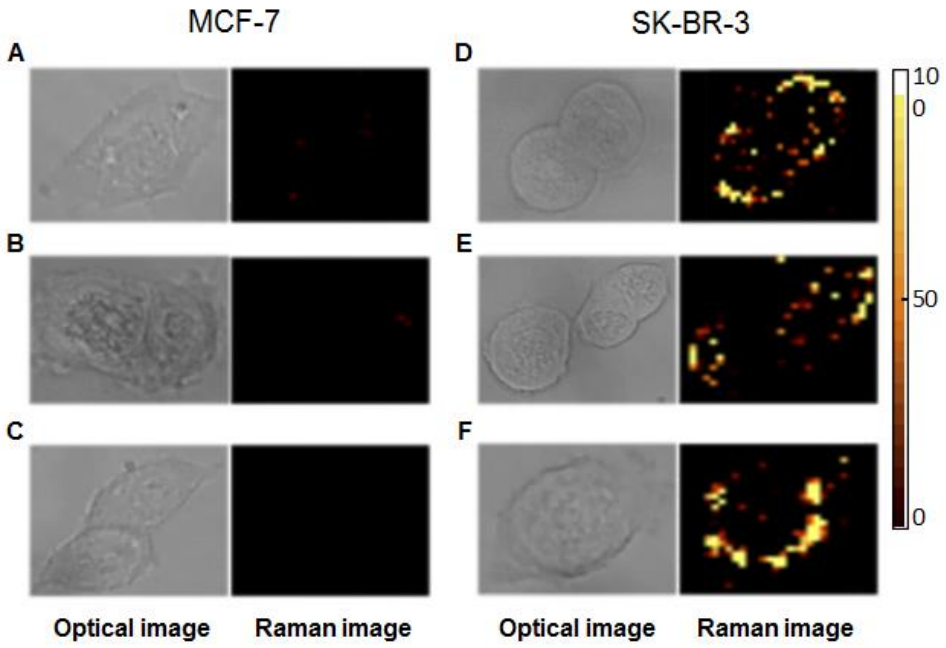

Figure 14. Selective detection of HER2-overexpressing cancer cells with SNA. (A)-(C) Optical images (left column) and Raman imaging (right column) was confirmed on MCF-7 cells as a negative control after treatment with SNA (10 mg/mL). (D)-(F) Optical images (left column) and Raman imaging (right column) was varified on SK-BR-3 cells expressing HER2 molecules after treatment with SNA (10 mg/mL).

DISCUSSION

Molecular imaging played important roles in biology and medicine owing to high spatial resolution and detection sensitivity. For long-term imaging and monitoring of fluorescently labeled substances was a major issue in fluorescence imaging because photo-bleaching was a major problem for most organic fluorescent dyes (131). And it arouse a high background of biological tissues. In recent years, carbon nanotubes have been explored in biological applications of sensing and detection and imaging (132). SNA was generated by nanotechnology designing, manufacturing and utilizing nanomaterials. To generate the SNA, SWNT synthesized with cotinine and then incubated with a bispecific antibody. As the bispecific antibody attached carbon nanotubes by the interaction of cotinine and anti-cotinine scFv, another sFv exposed more frequently. It was proved by BIAcore analysis measuring an affinity of SNA comparing with SWNT bioconjugates for HER2. SNA showed a much lower equilibrium dissociation constant (K_D) of 4.73×10^{-9} M than SWNT bioconjugate represented a K_D value of 1.54×10^{-6} M.

As SNA shown unique intrinsic optical properties and strong

resonance without photo-bleaching and background signal, it would be an ideal nanomaterial as biosensing and imaging platforms. The synthesized SNAs contaning anti-HER2 × cotinine antibody and anti-PSA × cotinine antibody showned a intensified Raman peak at 1593 cm^{-1} and 1583 cm^{-1}, respectively. Especially, SWNT with anti-HER2 × cotinine antibody represented meaningful valeus as an optical signal for detecting target molecues on cancer cells. In the Raman imaging, the specificity of SNA was proved by cell imaging for detection of HER2 molecules on SK-BR-3 cell surface. Herein, I suggest the SNA as a biomedical probe presenting a sensitivety and specificity as a diagnostic tool. Until now, the concentration of free PSAs such as [-2]proPSA, mature PSA and [-5/-7]proPSA in human serum was individually detected by ELISA for diagosing the protate cancer. As SNA could be generated with variant forms by adjusting C13/C12 isotope compositions (133), it is possible that SNA isotopes could be labeled with anti-[-2]proPSA antibody, anti-[-5/-7] antibody and anti-PSA antibody, respectively. SNA isotopes with different antibodies would be applied for detecting of free PSAs in human serum with a single tube. It will be next study

developing an assay for detecting various forms of free PSAs at the same time and study is ongoing.

REFERENCES

1. Mikolajczyk SD, Rittenhouse HG. Pro PSA: a more cancer specific form of prostate specific antigen for the early detection of prostate cancer. The Keio journal of medicine. 2003;52(2):86-91.
2. Hwang D, Yoon A, Kim S, Kim H, Chung J. Establishment of a mammalian expression system for recombinant [-2]proPSA and a specific antibody against the truncated leader peptide. Biotechnol Appl Biochem. 2016.
3. Kim HI, Hwang D, Jeon SJ, Lee S, Park JH, Yim D, et al. Orientation and density control of bispecific anti-HER2 antibody on functionalized carbon nanotubes for amplifying effective binding reactivity to cancer cells. Nanoscale. 2015;7(14):6363-73.
4. Ludwig JA, Weinstein JN. Biomarkers in cancer staging, prognosis and treatment selection. Nat Rev Cancer. 2005;5(11):845-56.
5. Yousef GM, Luo LY, Diamandis EP. Identification of novel human kallikrein-like genes on chromosome 19q13.3-q13.4. Anticancer Res. 1999;19(4B):2843-52.
6. Stenman UH, Leinonen J, Alfthan H, Rannikko S, Tuhkanen K, Alfthan O. A complex between prostate-specific antigen and alpha 1-antichymotrypsin is the major form of prostate-specific antigen in serum of patients with prostatic cancer: assay of the complex improves clinical sensitivity for cancer. Cancer Res. 1991;51(1):222-6.
7. Hsieh ML, Charlesworth MC, Goodmanson M, Zhang S, Seay T, Klee GG, et al. Expression of human prostate-specific glandular kallikrein protein (hK2) in the breast cancer cell line T47-D. Cancer Res. 1997;57(13):2651-6.
8. Peracaula R, Royle L, Tabares G, Mallorqui-Fernandez G, Barrabes S, Harvey DJ, et al. Glycosylation of human pancreatic ribonuclease: differences between normal and tumor states. Glycobiology. 2003;13(4):227-44.
9. Weir EG, Partin AW, Epstein JI. Correlation of serum prostate specific antigen and quantitative immunohistochemistry. The Journal of urology. 2000;163(6):1739-42.
10. Sozen S, Eskicorapci S, Kupeli B, Irkilata L, Altinel M, Ozer G, et al. Complexed prostate specific antigen density is better than the other PSA derivatives for detection of prostate cancer in men with total PSA between 2.5 and 20 ng/ml: results of a prospective multicenter study. European urology. 2005;47(3):302-7.
11. Kulasingam V, Diamandis EP. Strategies for discovering novel cancer biomarkers through utilization of emerging technologies. Nat Clin Pract Oncol. 2008;5(10):588-99.
12. Barry MJ. Clinical practice. Prostate-specific-antigen testing for early diagnosis of prostate cancer. The New England journal of medicine. 2001;344(18):1373-7.

13. Oesterling JE, Jacobsen SJ, Chute CG, Guess HA, Girman CJ, Panser LA, et al. Serum prostate-specific antigen in a community-based population of healthy men. Establishment of age-specific reference ranges. JAMA. 1993;270(7):860-4.
14. Polascik TJ, Oesterling JE, Partin AW. Prostate specific antigen: a decade of discovery--what we have learned and where we are going. The Journal of urology. 1999;162(2):293-306.
15. Bjurlin MA, Loeb S. PSA Velocity in Risk Stratification of Prostate Cancer. Rev Urol. 2013;15(4):204-6.
16. Seaman E, Whang M, Olsson CA, Katz A, Cooner WH, Benson MC. PSA density (PSAD). Role in patient evaluation and management. Urol Clin North Am. 1993;20(4):653-63.
17. Catalona WJ, Smith DS, Wolfert RL, Wang TJ, Rittenhouse HG, Ratliff TL, et al. Evaluation of percentage of free serum prostate-specific antigen to improve specificity of prostate cancer screening. JAMA. 1995;274(15):1214-20.
18. Catalona WJ, Southwick PC, Slawin KM, Partin AW, Brawer MK, Flanigan RC, et al. Comparison of percent free PSA, PSA density, and age-specific PSA cutoffs for prostate cancer detection and staging. Urology. 2000;56(2):255-60.
19. Bangma CH, Kranse R, Blijenberg BG, Schroder FH. The value of screening tests in the detection of prostate cancer. Part I: Results of a retrospective evaluation of 1726 men. Urology. 1995;46(6):773-8.
20. Luderer AA, Chen YT, Soriano TE, Kramp WJ, Carlson G, Cuny C, et al. Measurement of the Proportion of Free to Total Prostate-Specific Antigen Improves Diagnostic Performance of Prostate-Specific Antigen in the Diagnostic Gray Zone of Total Prostate-Specific Antigen. Urology. 1995;46(2):187-94.
21. Morgan TO, McLeod DG, Leifer ES, Murphy GP, Moul JW. Prospective use of free prostate-specific antigen to avoid repeat prostate biopsies in men with elevated total prostate-specific antigen. Urology. 1996;48(6A Suppl):76-80.
22. Hull D, Ma J, Singh H, Hossain D, Qian J, Bostwick DG. Precursor of prostate-specific antigen expression in prostatic intraepithelial neoplasia and adenocarcinoma: a study of 90 cases. BJU Int. 2009;104(7):915-8.
23. Mikolajczyk SD, Grauer LS, Millar LS, Hill TM, Kumar A, Rittenhouse HG, et al. A precursor form of PSA (pPSA) is a component of the free PSA in prostate cancer serum. Urology. 1997;50(5):710-4.
24. Hori S, Blanchet JS, McLoughlin J. From prostate-specific antigen (PSA) to precursor PSA (proPSA) isoforms: a review of the emerging role of proPSAs in the detection and management of early prostate cancer. BJU Int. 2013;112(6):717-28.
25. Lazzeri M, Haese A, Abrate A, de la Taille A, Redorta JP, McNicholas T, et al. Clinical performance of serum prostate-specific antigen isoform [-2]proPSA (p2PSA) and its derivatives, %p2PSA and

the prostate health index (PHI), in men with a family history of prostate cancer: results from a multicentre European study, the PROMEtheuS project. BJU Int. 2013;112(3):313-21.
26. Wang L, Zhao WJ, Tan WH. Bioconjugated Silica Nanoparticles: Development and Applications. Nano Research. 2008;1(2):99-115.
27. Dai H. Carbon nanotubes: synthesis, integration, and properties. Acc Chem Res. 2002;35(12):1035-44.
28. Munge B, Liu GD, Collins G, Wang J. Multiple enzyme layers on carbon nanotubes for electrochemical detection down to 80 DNA copies. Analytical Chemistry. 2005;77(14):4662-6.
29. Iijima S, Ichihashi T. Single-Shell Carbon Nanotubes of 1-Nm Diameter (Vol 363, Pg 603, 1993). Nature. 1993;364(6439):737-.
30. Iijima S. Helical Microtubules of Graphitic Carbon. Nature. 1991;354(6348):56-8.
31. Lee J, Mahendra S, Alvarez PJJ. Nanomaterials in the Construction Industry: A Review of Their Applications and Environmental Health and Safety Considerations. Acs Nano. 2010;4(7):3580-90.
32. Journet C, Maser WK, Bernier P, Loiseau A, delaChapelle ML, Lefrant S, et al. Large-scale production of single-walled carbon nanotubes by the electric-arc technique. Nature. 1997;388(6644):756-8.
33. Kim P, Odom TW, Huang JL, Lieber CM. Electronic density of states of atomically resolved single-walled carbon nanotubes: Van Hove singularities and end states. Phys Rev Lett. 1999;82(6):1225-8.
34. Jorio A, Pimenta MA, Souza AG, Saito R, Dresselhaus G, Dresselhaus MS. Characterizing carbon nanotube samples with resonance Raman scattering. New J Phys. 2003;5.
35. Dresselhaus MS, Dresselhaus G, Saito R, Jorio A. Raman spectroscopy of carbon nanotubes. Phys Rep. 2005;409(2):47-99.
36. Chen Z, Tabakman SM, Goodwin AP, Kattah MG, Daranciang D, Wang XR, et al. Protein microarrays with carbon nanotubes as multicolor Raman labels. Nature Biotechnology. 2008;26(11):1285-92.
37. Liu ZA, Li XL, Tabakman SM, Jiang KL, Fan SS, Dai HJ. Multiplexed multicolor Raman imaging of live cells with isotopically modified single walled carbon nanotubes. J Am Chem Soc. 2008;130(41):13540-+.
38. Liu Z, Davis C, Cai WB, He L, Chen XY, Dai HJ. Circulation and long-term fate of functionalized, biocompatible single-walled carbon nanotubes in mice probed by Raman spectroscopy. P Natl Acad Sci USA. 2008;105(5):1410-5.
39. Peracaula R, Tabares G, Royle L, Harvey DJ, Dwek RA, Rudd PM, et al. Altered glycosylation pattern allows the distinction between prostate-specific antigen (PSA) from normal and tumor origins. Glycobiology. 2003;13(6):457-70.
40. Weir EG, Partin AW, Epstein JI. Correlation of serum prostate

specific antigen and quantitative immunohistochemistry. J Urology. 2000;163(6):1739-42.
41. Ozen H, Sozen S. PSA isoforms in prostate cancer detection. Eur Urol Suppl. 2006;5(6):495-9.
42. Catalona WJ, Smith DS, Ratliff TL, Dodds KM, Coplen DE, Yuan JJ, et al. Measurement of prostate-specific antigen in serum as a screening test for prostate cancer. The New England journal of medicine. 1991;324(17):1156-61.
43. Hugosson J, Carlsson S, Aus G, Bergdahl S, Khatami A, Lodding P, et al. Mortality results from the Goteborg randomised population-based prostate-cancer screening trial. The Lancet Oncology. 2010;11(8):725-32.
44. Schroder FH, Hugosson J, Roobol MJ, Tammela TL, Ciatto S, Nelen V, et al. Prostate-cancer mortality at 11 years of follow-up. The New England journal of medicine. 2012;366(11):981-90.
45. Thompson IM, Pauler DK, Goodman PJ, Tangen CM, Lucia MS, Parnes HL, et al. Prevalence of prostate cancer among men with a prostate-specific antigen level <= 4.0 ng per milliliter. New Engl J Med. 2004;350(22):2239-46.
46. Gilgunn S, Conroy PJ, Saldova R, Rudd PM, O'Kennedy RJ. Aberrant PSA glycosylation--a sweet predictor of prostate cancer. Nat Rev Urol. 2013;10(2):99-107.
47. Emiliozzi P, Longhi S, Scarpone P, Pansadoro A, DePaula F, Pansadoro V. The value of a single biopsy with 12 transperineal cores for detecting prostate cancer in patients with elevated prostate specific antigen. The Journal of urology. 2001;166(3):845-50.
48. Chan TY, Mikolajczyk SD, Lecksell K, Shue MJ, Rittenhouse HG, Partin AW, et al. Immunohistochemical staining of prostate cancer with monoclonal antibodies to the precursor of prostate-specific antigen. Urology. 2003;62(1):177-81.
49. Sokoll LJ, Sanda MG, Feng Z, Kagan J, Mizrahi IA, Broyles DL, et al. A prospective, multicenter, National Cancer Institute Early Detection Research Network study of [-2]proPSA: improving prostate cancer detection and correlating with cancer aggressiveness. Cancer Epidemiol Biomarkers Prev. 2010;19(5):1193-200.
50. Stephan C, Kahrs AM, Cammann H, Lein M, Schrader M, Deger S, et al. A [-2]proPSA-based artificial neural network significantly improves differentiation between prostate cancer and benign prostatic diseases. The Prostate. 2009;69(2):198-207.
51. Makarov DV, Isharwal S, Sokoll LJ, Landis P, Marlow C, Epstein JI, et al. Pro-prostate-specific antigen measurements in serum and tissue are associated with treatment necessity among men enrolled in expectant management for prostate cancer. Clinical cancer research : an official journal of the American Association for Cancer Research. 2009;15(23):7316-21.
52. Carlos F. Barbas III DRB, Jamie K. Scott, Gregg J. Silverman.

Phage Display - A Laboratory Manual. New York: Cold Spring Harbor Laboratory Press; 2001.
53. Smith GP. Filamentous Fusion Phage - Novel Expression Vectors That Display Cloned Antigens on the Virion Surface. Science. 1985;228(4705):1315-7.
54. Bass S, Greene R, Wells JA. Hormone Phage - an Enrichment Method for Variant Proteins with Altered Binding-Properties. Proteins. 1990;8(4):309-14.
55. Huston JS, Levinson D, Mudgetthunter M, Tai MS, Novotny J, Margolies MN, et al. Protein Engineering of Antibody-Binding Sites - Recovery of Specific Activity in an Anti-Digoxin Single-Chain Fv Analog Produced in Escherichia-Coli. P Natl Acad Sci USA. 1988;85(16):5879-83.
56. Bird RE, Hardman KD, Jacobson JW, Johnson S, Kaufman BM, Lee SM, et al. Single-Chain Antigen-Binding Proteins. Science. 1988;242(4877):423-6.
57. Mccafferty J, Griffiths AD, Winter G, Chiswell DJ. Phage Antibodies - Filamentous Phage Displaying Antibody Variable Domains. Nature. 1990;348(6301):552-4.
58. Hoogenboom HR, Griffiths AD, Johnson KS, Chiswell DJ, Hudson P, Winter G. Multi-subunit proteins on the surface of filamentous phage: methodologies for displaying antibody (Fab) heavy and light chains. Nucleic Acids Res. 1991;19(15):4133-7.
59. Garrard LJ, Yang M, O'Connell MP, Kelley RF, Henner DJ. Fab assembly and enrichment in a monovalent phage display system. Biotechnology (N Y). 1991;9(12):1373-7.
60. Breitling F, Dubel S, Seehaus T, Klewinghaus I, Little M. A surface expression vector for antibody screening. Gene. 1991;104(2):147-53.
61. Bass S, Greene R, Wells JA. Hormone phage: an enrichment method for variant proteins with altered binding properties. Proteins. 1990;8(4):309-14.
62. Barbas CF, 3rd, Kang AS, Lerner RA, Benkovic SJ. Assembly of combinatorial antibody libraries on phage surfaces: the gene III site. Proc Natl Acad Sci U S A. 1991;88(18):7978-82.
63. Iliichev AA, Minenkova OO, Tatkov SI, Karpyshev NN, Eroshkin AM, Petrenko VA, et al. Production of the M13 Phage Viable Variant with a Foreign Peptide Inserted into the Coat Basic-Protein. Dokl Akad Nauk Sssr+ . 1989;307(2):481-3.
64. Greenwood J, Willis AE, Perham RN. Multiple Display of Foreign Peptides on a Filamentous Bacteriophage - Peptides from Plasmodium-Falciparum Circumsporozoite Protein as Antigens. Journal of Molecular Biology. 1991;220(4):821-7.
65. Cabilly S. The basic structure of filamentous phage and its use in the display of combinatorial peptide libraries. Mol Biotechnol. 1999;12(2):143-8.

66. Pluckthun A. Antibody engineering. Curr Opin Biotechnol. 1991;2(2):238-46.
67. Chang CN, Landolfi NF, Queen C. Expression of antibody Fab domains on bacteriophage surfaces. Potential use for antibody selection. J Immunol. 1991;147(10):3610-4.
68. Felici F, Castagnoli L, Musacchio A, Jappelli R, Cesareni G. Selection of Antibody Ligands from a Large Library of Oligopeptides Expressed on a Multivalent Exposition Vector. Journal of Molecular Biology. 1991;222(2):301-10.
69. Barbas CF, Kang AS, Lerner RA, Benkovic SJ. Assembly of Combinatorial Antibody Libraries on Phage Surfaces - the Gene-Iii Site. P Natl Acad Sci USA. 1991;88(18):7978-82.
70. Marks JD, Ouwehand WH, Bye JM, Finnern R, Gorick BD, Voak D, et al. Human antibody fragments specific for human blood group antigens from a phage display library. Biotechnology (N Y). 1993;11(10):1145-9.
71. Hawkins RE, Russell SJ, Winter G. Selection of Phage Antibodies by Binding-Affinity - Mimicking Affinity Maturation. Journal of Molecular Biology. 1992;226(3):889-96.
72. Marks JD, Hoogenboom HR, Bonnert TP, Mccafferty J, Griffiths AD, Winter G. By-Passing Immunization - Human-Antibodies from V-Gene Libraries Displayed on Phage. Journal of Molecular Biology. 1991;222(3):581-97.
73. Milstein C. The Croonian Lecture, 1989 - Antibodies - a Paradigm for the Biology of Molecular Recognition. Proc R Soc Ser B-Bio. 1990;239(1294):1-16.
74. Garrard LJ, Yang M, Oconnell MP, Kelley RF, Henner DJ. Fab Assembly and Enrichment in a Monovalent Phage Display System. Bio-Technol. 1991;9(12):1373-7.
75. Griffiths AD, Williams SC, Hartley O, Tomlinson IM, Waterhouse P, Crosby WL, et al. Isolation of High-Affinity Human-Antibodies Directly from Large Synthetic Repertoires. Embo J. 1994;13(14):3245-60.
76. de Haard HJ, van Neer N, Reurs A, Hufton SE, Roovers RC, Henderikx P, et al. A large non-immunized human Fab fragment phage library that permits rapid isolation and kinetic analysis of high affinity antibodies. J Biol Chem. 1999;274(26):18218-30.
77. Knappik A, Ge LM, Honegger A, Pack P, Fischer M, Wellnhofer G, et al. Fully synthetic human combinatorial antibody libraries (HuCAL) based on modular consensus frameworks and CDRs randomized with trinucleotides. Journal of Molecular Biology. 2000;296(1):57-86.
78. Lu D, Shen JQ, Vil MD, Zhang HF, Jimenez X, Bohlen P, et al. Tailoring in vitro selection for a picomolar affinity human antibody directed against vascular endothelial growth factor receptor 2 for enhanced neutralizing activity. J Biol Chem. 2003;278(44):43496-507.
79. Kramer RA, Marissen WE, Goudsmit J, Visser TJ, Clijsters-Van

der Horst M, Bakker AQ, et al. The human antibody repertoire specific for rabies virus glycoprotein as selected from immune libraries. Eur J Immunol. 2005;35(7):2131-45.
80. Lee Y, Kim H, Chung J. An antibody reactive to the Gly63-Lys68 epitope of NT-proBNP exhibits O-glycosylation-independent binding. Experimental & molecular medicine. 2014;46:e114.
81. Reed SE, Staley EM, Mayginnes JP, Pintel DJ, Tullis GE. Transfection of mammalian cells using linear polyethylenimine is a simple and effective means of producing recombinant adeno-associated virus vectors. J Virol Methods. 2006;138(1-2):85-98.
82. Diezel W, Kopperschlager G, Hofmann E. An improved procedure for protein staining in polyacrylamide gels with a new type of Coomassie Brilliant Blue1972 Aug. 617-20 p.
83. Paraiso KH, Van Der Kooi K, Messina JL, Smalley KS. Measurement of constitutive MAPK and PI3K/AKT signaling activity in human cancer cell lines. Methods Enzymol. 2010;484:549-67.
84. Hara K, Shiota M, Kido H, Ohtsu Y, Kashiwagi T, Iwahashi J, et al. Influenza virus RNA polymerase PA subunit is a novel serine protease with Ser624 at the active site. Genes Cells. 2001;6(2):87-97.
85. Andrews GL, Simons BL, Young JB, Hawkridge AM, Muddiman DC. Performance characteristics of a new hybrid quadrupole time-of-flight tandem mass spectrometer (TripleTOF 5600). Anal Chem. 2011;83(13):5442-6.
86. Hong P, Koza S, Bouvier ES. Size-Exclusion Chromatography for the Analysis of Protein Biotherapeutics and their Aggregates. J Liq Chromatogr Relat Technol. 2012;35(20):2923-50.
87. Vessely C, Estey T, Randolph TW, Henderson I, Nayar R, Carpenter JF. Effects of solution conditions and surface chemistry on the adsorption of three recombinant botulinum neurotoxin antigens to aluminum salt adjuvants. J Pharm Sci. 2007;96(9):2375-89.
88. Lee MS, Lee JC, Choi CY, Chung J. Production and characterization of monoclonal antibody to botulinum neurotoxin type B light chain by phage display. Hybridoma (Larchmt). 2008;27(1):18-24.
89. Barbas CF III BD, Scott JK and Silverman GJ. Phage Display - A Laboratory Manual. Cold Spring Harbor Laboratory Press, New York, USA2001.
90. Park S, Lee DH, Park JG, Lee YT, Chung J. A sensitive enzyme immunoassay for measuring cotinine in passive smokers. Clin Chim Acta. 2010;411(17-18):1238-42.
91. Miyashita M, Presley JM, Buchholz BA, Lam KS, Lee YM, Vogel JS, et al. Attomole level protein sequencing by Edman degradation coupled with accelerator mass spectrometry. Proc Natl Acad Sci U S A. 2001;98(8):4403-8.
92. Vilaseca C, Quintana MC, Hernandez P, Vicente J, Hernandez L. Analysis of PTH-Cysteine by Adsorptive Stripping Square-Wave Voltammetry. Electroanal. 2009;21(3-5):459-63.

93. Chen X, Flynn GC. Analysis of N-glycans from recombinant immunoglobulin G by on-line reversed-phase high-performance liquid chromatography/mass spectrometry. Anal Biochem. 2007;370(2):147-61.
94. Garcia BA, Shabanowitz J, Hunt DF. Analysis of protein phosphorylation by mass spectrometry. Methods. 2005;35(3):256-64.
95. Jenkins N, Meleady P, Tyther R, Murphy L. Strategies for analysing and improving the expression and quality of recombinant proteins made in mammalian cells. Biotechnol Appl Biochem. 2009;53(Pt 2):73-83.
96. Sokoll LJ, Wang Y, Feng Z, Kagan J, Partin AW, Sanda MG, et al. [-2]proenzyme prostate specific antigen for prostate cancer detection: a national cancer institute early detection research network validation study. The Journal of urology. 2008;180(2):539-43; discussion 43.
97. Guazzoni G, Nava L, Lazzeri M, Scattoni V, Lughezzani G, Maccagnano C, et al. Prostate-specific antigen (PSA) isoform p2PSA significantly improves the prediction of prostate cancer at initial extended prostate biopsies in patients with total PSA between 2.0 and 10 ng/ml: results of a prospective study in a clinical setting. European urology. 2011;60(2):214-22.
98. Mikolajczyk SD, Marker KM, Millar LS, Kumar A, Saedi MS, Payne JK, et al. A truncated precursor form of prostate-specific antigen is a more specific serum marker of prostate cancer. Cancer Res. 2001;61(18):6958-63.
99. Naya Y, Fritsche HA, Bhadkamkar VA, Mikolajczyk SD, Rittenhouse HG, Babaian RJ. Evaluation of precursor prostate-specific antigen isoform ratios in the detection of prostate cancer. Urologic oncology. 2005;23(1):16-21.
100. Sokoll LJ, Chan DW, Klee GG, Roberts WL, van Schaik RH, Arockiasamy DA, et al. Multi-center analytical performance evaluation of the Access Hybritech(R) p2PSA immunoassay. Clin Chim Acta. 2012;413(15-16):1279-83.
101. Liu Z, Cai W, He L, Nakayama N, Chen K, Sun X, et al. In vivo biodistribution and highly efficient tumour targeting of carbon nanotubes in mice. Nat Nanotechnol. 2007;2(1):47-52.
102. Heller DA, Jeng ES, Yeung TK, Martinez BM, Moll AE, Gastala JB, et al. Optical detection of DNA conformational polymorphism on single-walled carbon nanotubes. Science. 2006;311(5760):508-11.
103. Kim JH, Heller DA, Jin H, Barone PW, Song C, Zhang J, et al. The rational design of nitric oxide selectivity in single-walled carbon nanotube near-infrared fluorescence sensors for biological detection. Nat Chem. 2009;1(6):473-81.
104. Kim JH, Ahn JH, Barone PW, Jin H, Zhang J, Heller DA, et al. A luciferase/single-walled carbon nanotube conjugate for near-infrared fluorescent detection of cellular ATP. Angew Chem Int Ed Engl.

2010;49(8):1456-9.
105. Chen Z, Tabakman SM, Goodwin AP, Kattah MG, Daranciang D, Wang X, et al. Protein microarrays with carbon nanotubes as multicolor Raman labels. Nat Biotechnol. 2008;26(11):1285-92.
106. Zavaleta C, de la Zerda A, Liu Z, Keren S, Cheng Z, Schipper M, et al. Noninvasive Raman spectroscopy in living mice for evaluation of tumor targeting with carbon nanotubes. Nano Lett. 2008;8(9):2800-5.
107. Gao X, Cui Y, Levenson RM, Chung LW, Nie S. In vivo cancer targeting and imaging with semiconductor quantum dots. Nat Biotechnol. 2004;22(8):969-76.
108. Aubin-Tam ME, Hamad-Schifferli K. Structure and function of nanoparticle-protein conjugates. Biomed Mater. 2008;3(3):034001.
109. Medintz I. Universal tools for biomolecular attachment to surfaces. Nat Mater. 2006;5(11):842.
110. Shaw SY, Westly EC, Pittet MJ, Subramanian A, Schreiber SL, Weissleder R. Perturbational profiling of nanomaterial biologic activity. Proc Natl Acad Sci U S A. 2008;105(21):7387-92.
111. Xing Y, Chaudry Q, Shen C, Kong KY, Zhau HE, Chung LW, et al. Bioconjugated quantum dots for multiplexed and quantitative immunohistochemistry. Nat Protoc. 2007;2(5):1152-65.
112. Diamandis EP, Christopoulos TK. The biotin-(strept)avidin system: principles and applications in biotechnology. Clin Chem. 1991;37(5):625-36.
113. Mamidyala SK, Finn MG. In situ click chemistry: probing the binding landscapes of biological molecules. Chem Soc Rev. 2010;39(4):1252-61.
114. Haun JB, Devaraj NK, Hilderbrand SA, Lee H, Weissleder R. Bioorthogonal chemistry amplifies nanoparticle binding and enhances the sensitivity of cell detection. Nat Nanotechnol. 2010;5(9):660-5.
115. Xu CJ, Xu KM, Gu HW, Zhong XF, Guo ZH, Zheng RK, et al. Nitrilotriacetic acid-modified magnetic nanoparticles as a general agent to bind histidine-tagged proteins. J Am Chem Soc. 2004;126(11):3392-3.
116. Ahn JH, Kim JH, Reuel NF, Barone PW, Boghossian AA, Zhang J, et al. Label-free, single protein detection on a near-infrared fluorescent single-walled carbon nanotube/protein microarray fabricated by cell-free synthesis. Nano Lett. 2011;11(7):2743-52.
117. Mazzucchelli S, Colombo M, Verderio P, Rozek E, Andreata F, Galbiati E, et al. Orientation-controlled conjugation of haloalkane dehalogenase fused homing peptides to multifunctional nanoparticles for the specific recognition of cancer cells. Angew Chem Int Ed Engl. 2013;52(11):3121-5.
118. Colombo M, Mazzucchelli S, Montenegro JM, Galbiati E, Corsi F, Parak WJ, et al. Protein oriented ligation on nanoparticles exploiting O6-alkylguanine-DNA transferase (SNAP) genetically encoded fusion. Small. 2012;8(10):1492-7.

119. Li QW, Zhang XF, DePaula RF, Zheng LX, Zhao YH, Stan L, et al. Sustained growth of ultralong carbon nanotube arrays for fiber spinning. Adv Mater. 2006;18(23):3160-+.
120. O'Connell MJ, Bachilo SM, Huffman CB, Moore VC, Strano MS, Haroz EH, et al. Band gap fluorescence from individual single-walled carbon nanotubes. Science. 2002;297(5581):593-6.
121. Bachilo SM, Strano MS, Kittrell C, Hauge RH, Smalley RE, Weisman RB. Structure-assigned optical spectra of single-walled carbon nanotubes. Science. 2002;298(5602):2361-6.
122. Cherukuri P, Bachilo SM, Litovsky SH, Weisman RB. Near-infrared fluorescence microscopy of single-walled carbon nanotubes in phagocytic cells. J Am Chem Soc. 2004;126(48):15638-9.
123. Riah O, Dousset JC, Courriere P, Stigliani JL, Baziard-Mouysset G, Belahsen Y. Evidence that nicotine acetylcholine receptors are not the main targets of cotinine toxicity. Toxicol Lett. 1999;109(1-2):21-9.
124. Nian H, Wang J, Wu H, Lo JG, Chiu KH, Pounds JG, et al. Electrochemical immunoassay of cotinine in serum based on nanoparticle probe and immunochromatographic strip. Anal Chim Acta. 2012;713:50-5.
125. Barone PW, Strano MS. Reversible control of carbon nanotube aggregation for a glucose affinity sensor. Angew Chem Int Edit. 2006;45(48):8138-41.
126. Carlsson J, Nordgren H, Sjostrom J, Wester K, Villman K, Bengtsson NO, et al. HER2 expression in breast cancer primary tumours and corresponding metastases. Original data and literature review. Br J Cancer. 2004;90(12):2344-8.
127. Lattrich C, Juhasz-Boess I, Ortmann O, Treeck O. Detection of an elevated HER2 expression in MCF-7 breast cancer cells overexpressing estrogen receptor beta1. Oncol Rep. 2008;19(3):811-7.
128. Luo J, Zhou J, Zou W, Shen P. Antibody-antigen interactions measured by surface plasmon resonance: global fitting of numerical integration algorithms. J Biochem. 2001;130(4):553-9.
129. Katz E, Willner I. Integrated nanoparticle-biomolecule hybrid systems: synthesis, properties, and applications. Angew Chem Int Ed Engl. 2004;43(45):6042-108.
130. Davis ME, Chen ZG, Shin DM. Nanoparticle therapeutics: an emerging treatment modality for cancer. Nat Rev Drug Discov. 2008;7(9):771-82.
131. Song L, Hennink EJ, Young IT, Tanke HJ. Photobleaching kinetics of fluorescein in quantitative fluorescence microscopy. Biophys J. 1995;68(6):2588-600.
132. Welsher K, Liu Z, Daranciang D, Dai H. Selective probing and imaging of cells with single walled carbon nanotubes as near-infrared fluorescent molecules. Nano Lett. 2008;8(2):586-90.
133. Liu Z, Tabakman S, Sherlock S, Li X, Chen Z, Jiang K, et al.

Multiplexed Five-Color Molecular Imaging of Cancer Cells and Tumor Tissues with Carbon Nanotube Raman Tags in the Near-Infrared. Nano Res. 2010;3(3):222-33.

국문 초록

서론: 전립선 암을 진단하는 방법 중 하나로서 사람 혈청 내 존재하는 Free PSA, complex PSA 를 측정하는 방법이 있다. 최근 들어, 이들 단백질의 전구체인 proPSA 가 free PSA 나 complex PSA 보다 전립선 암을 정확하게 진단하는데 유용하다고 보고되고 있으며 전립선암 특이적 마커로서 [-2]proPSA, [-5/-7]proPSA 에 대한 연구가 활발히 이루어지고 있다. 또한 최근 연구 동향에 따르면, 항체공학과 나노테크놀로지를 접목시켜 전립선암을 진단하는 방법에 대한 연구가 활발히 이루어지고 있다.

방법: 본 연구에서는 proPSA 를 HEK293F 세포에서 발현 및 정제하였다. proPSA 는 단백질 아미노말단 서열분석 및 질량분석법을 통하여 단백질을 분석하였다. 아미노말단 서열이 확인된 proPSA 단백질과 펩타이드-컨쥬게이트를 각각 닭에 면역하였으며, 닭 혈청 내 항체 역가는 면역블롯을 통하여 측정하였다. 닭의 조직으로부터 구축한 파지 라이브러리는 panning 과정을 거쳐 [-2]proPSA, [-5/-7]proPSA 특이적인 항체들를 선별하였다. 선별된 항체들의 항원에 대한 특이성 및 결합도는 효소분석법을 통하여 측정하였다. 이와 더불어 본 연구진은 a-HER2 × cotinie 항체, a-PSA ×

cotinine 항체를 발현 및 정제하였으며 라만분석법을 통하여 이들 항체가 접합된 카본나노튜브의 특성을 분석하였다.

결과: 파지 디스플레이기법을 통하여[−2]proPSA, [−5/−7]proPSA 단백질과 펩타이드−컨쥬게이트 면역 라이브러리로부터 [−2]proPSA, [−5/−7]proPSA 의 아미노말단 서열에 특이적인 항체를 발굴하였다. 발굴한 항체의 항원결합부위를 분석한 결과 항−[−2]proPSA 항체는 아미노 말단에 존재하는 세린 잔기에 특이적으로 붙는 것을 확인하였으며, 항−[−5/−7]proPSA 항체는 아미노 말단에 존재하는 루이신 잔기가 항원결합부위임을 밝혀냈다. 또한 라만 스펙트럼을 통하여 이중특이성항체와 카본나노튜브 접합체를 분석한 결과, 개발한 생체 프로브가 항원에 특이적으로 결합하는 것을 세포 이미징 기법을 통하여 확인하였다.

결론: 본 연구에서는 [−2]proPSA, [−5/−7]proPSA 의 아미노말단 서열에 특이적으로 결합하는 항체와 더불어 이중특이성항체와 카본나노튜브 접합체라는 새로운 생체 프로브를 개발하였다. 발굴한 항체와 생체 프로부는 향후, 바이오메디컬 센서로서 전립선암을 진단하는데 적용 가능할 것이라 보여진다.

주요어 : **proPSA, 전립선암, 코티닌, 항체, 카본나노튜브 접합체, Raman**

학 번 : **2008-23299**